Introduction to EM

INSTITUTE OF PHYSICS OF MATERIALS
Czech Academy of Sciences

Light microscopy - limitation

resolution

magnification

depth of focus

$$d_d = 0.61\,\lambda / \alpha$$

Abbe, Airy

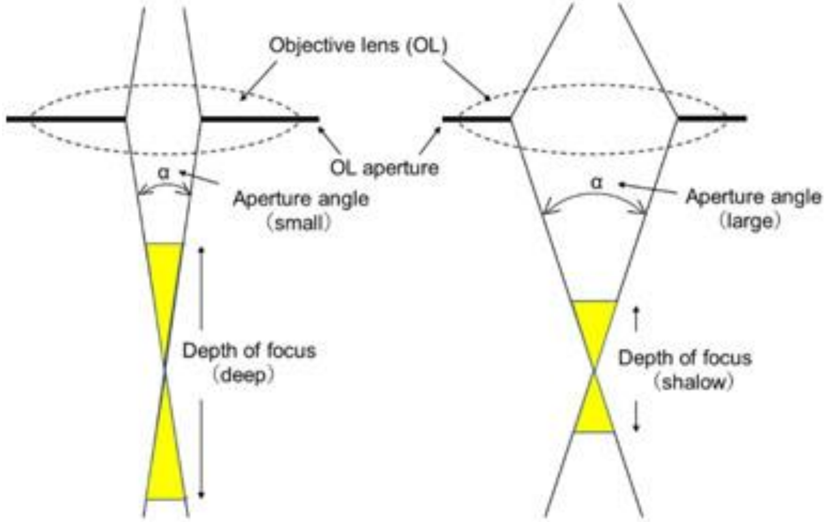

visible light - > λ = 390 – 760 nm

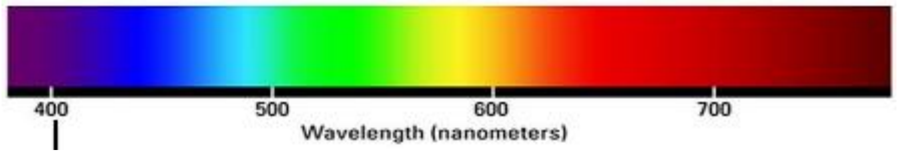

Table Electron Properties as a Function of Accelerating Voltage

Accelerating voltage (kV)	Nonrelativistic wavelength (nm)	Relativistic wavelength (nm)	Mass ($\times m_0$)	Velocity ($\times 10^8$ m/s)
100	0.00386	0.00370	1.196	1.644
120	0.00352	0.00335	1.235	1.759
200	0.00273	0.00251	1.391	2.086
300	0.00223	0.00197	1.587	2.330
400	0.00193	0.00164	1.783	2.484
1000	0.00122	0.00087	2.957	2.823

$$\lambda = \frac{h}{\sqrt{2m_0eU\left(1+\frac{eU}{m_0c^2}\right)}} \approx \frac{h}{\sqrt{2m_0eU}} \Rightarrow \boldsymbol{\lambda = \frac{1,226}{\sqrt{U}}}\,[nm]$$

U=10kV (SEM) -> **λ = 0.01226 nm**
U=100kV (TEM) -> **λ = 0.0039 nm**
Visible light - > λ = 390 – 760 nm

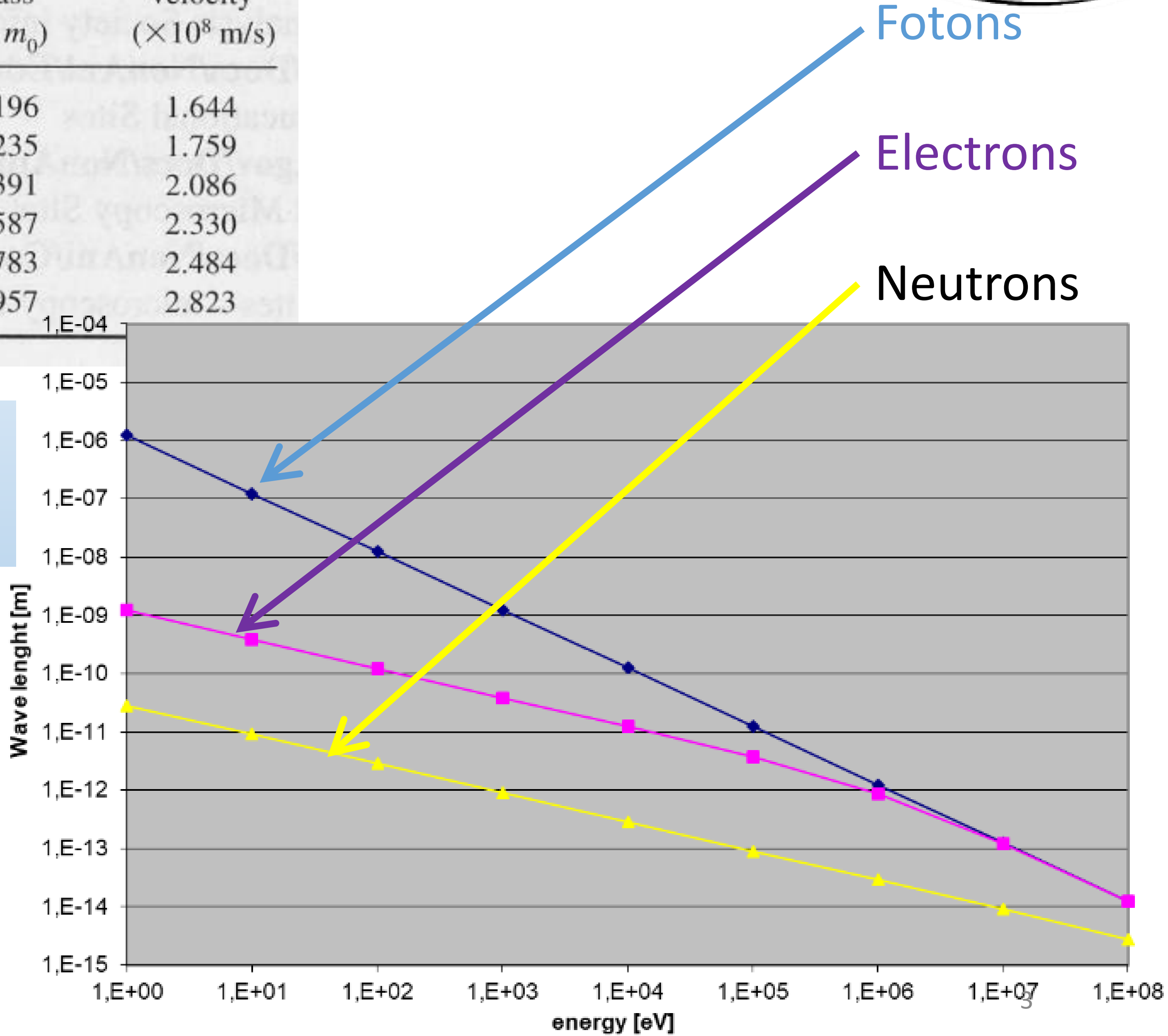

Electron microscopy

SEM

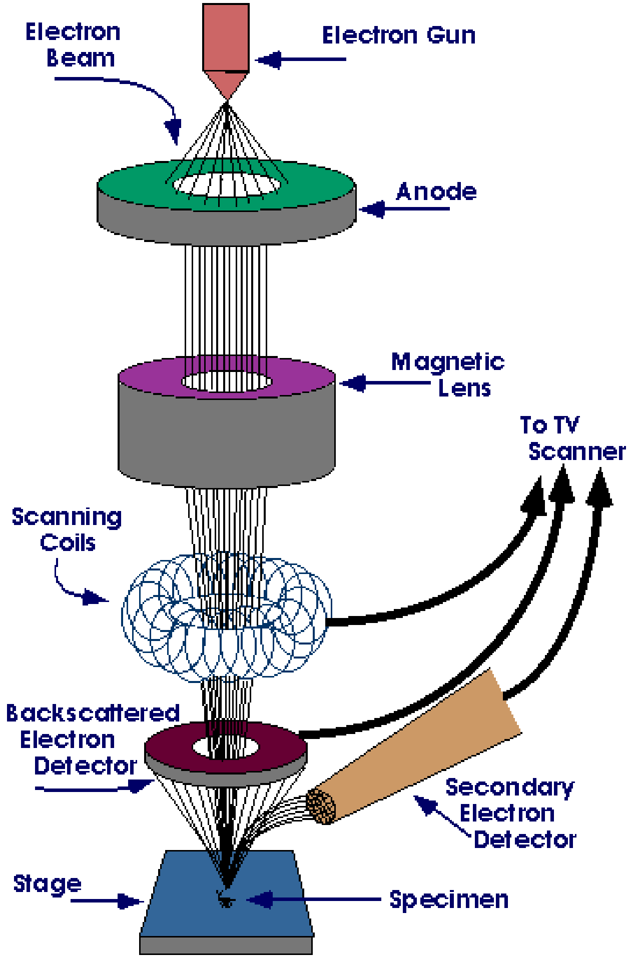

TEM

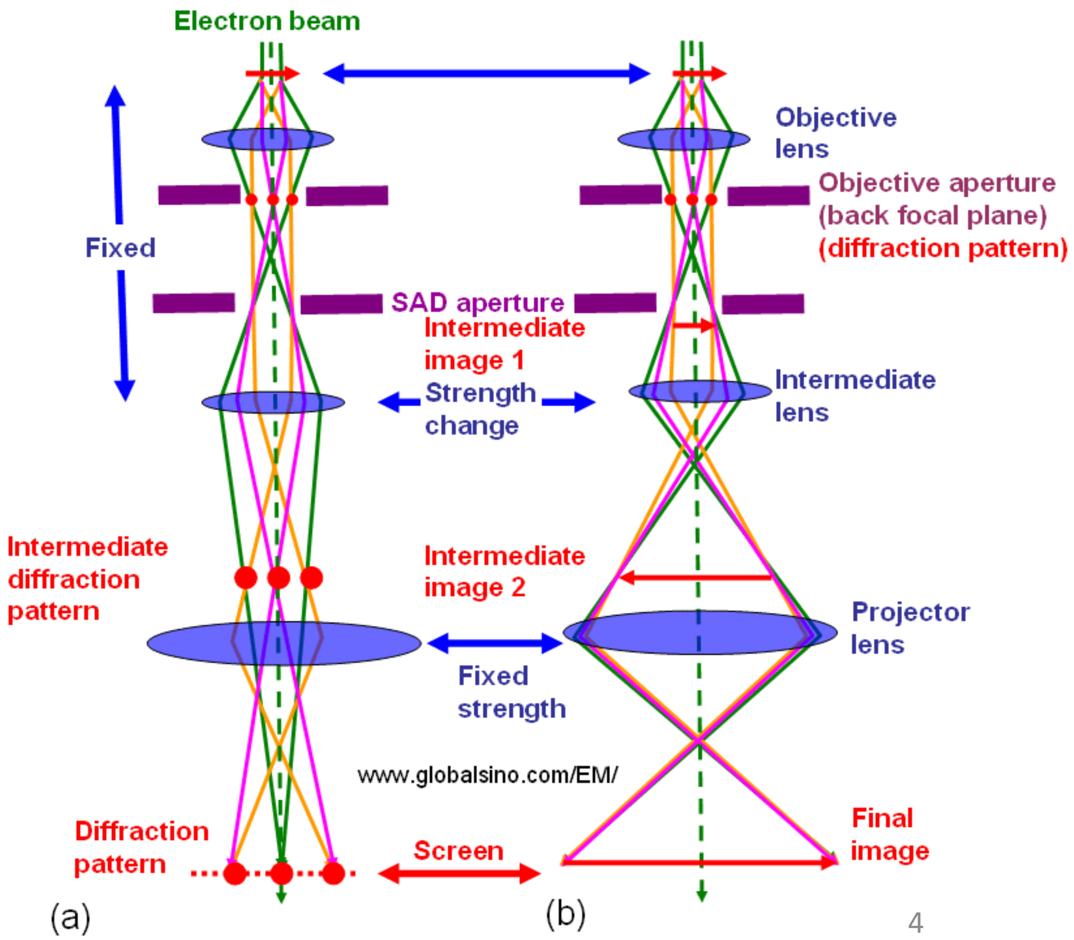

Specimens

SEM

Conductive specimens! (C, Au coatings)

Polished or electropolished metalographic cuts

Fracture surfaces

Tensile, fatigue, creep,… specimens

Powders

TEM

Specimens transparent for electrons! (~ 100 nm)

Thin foils – electropolished, Ar ions bombardment

Surface or extraction replica

Nanopowders

FIB

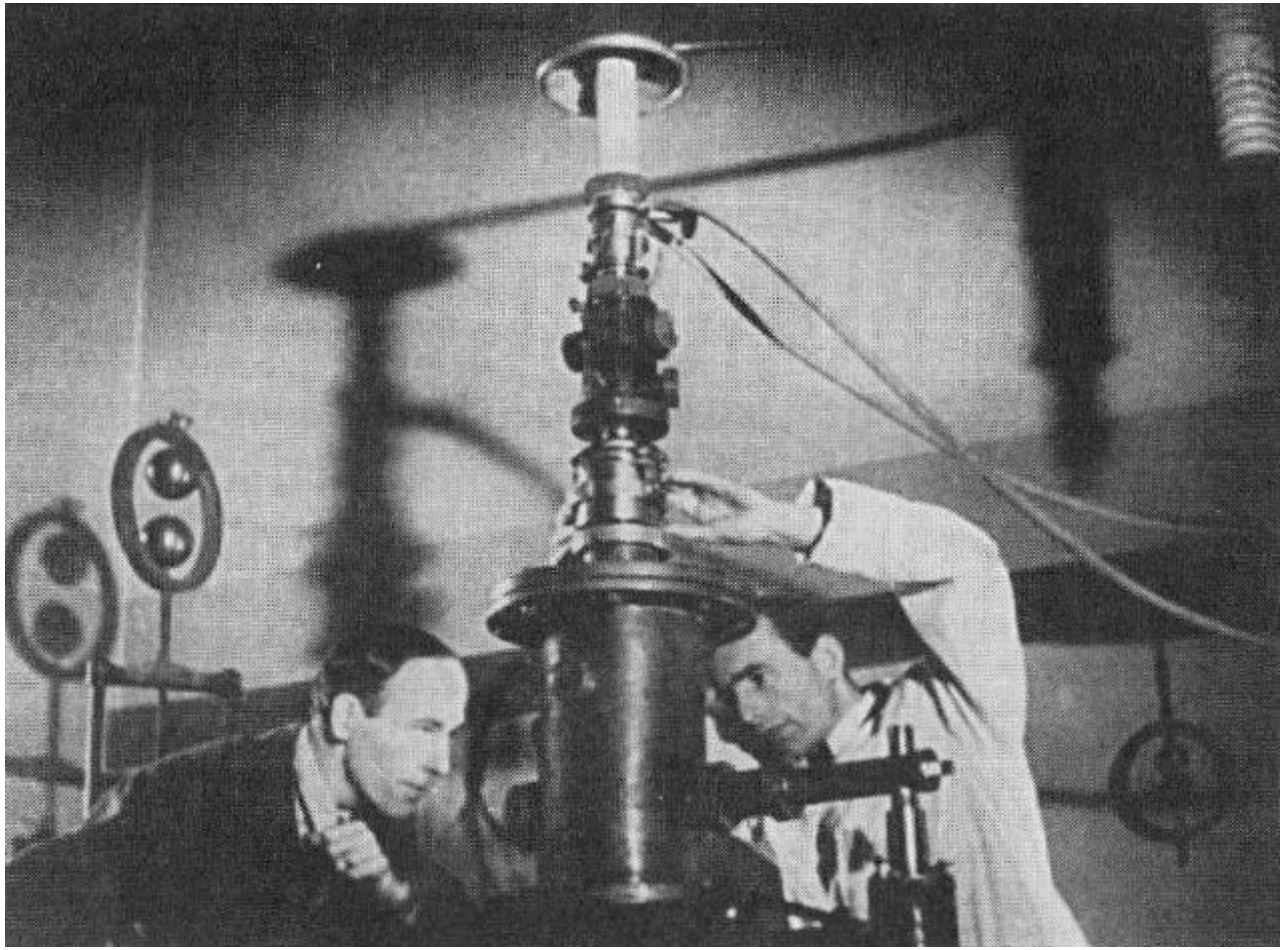

Berlin early 1930s: Ruska and Knoll

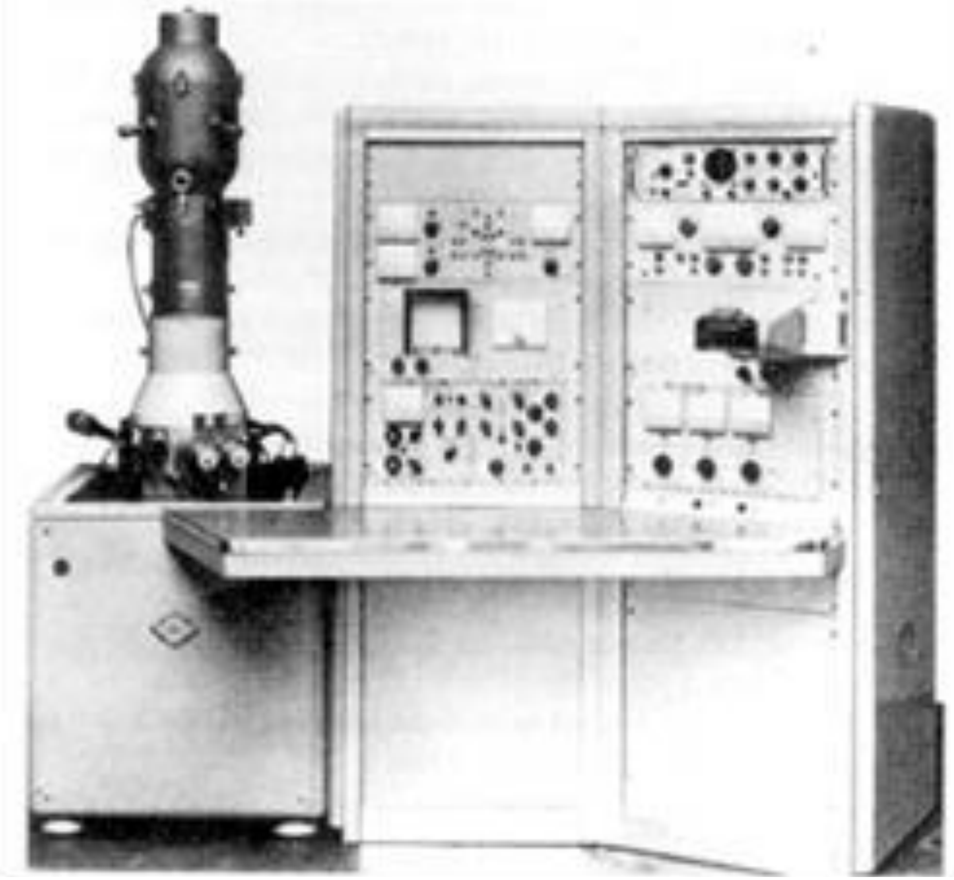

1931: 16x

1933: 12000x

1965: Oatley, first commercial SEM Stereoscan

Vacuum system

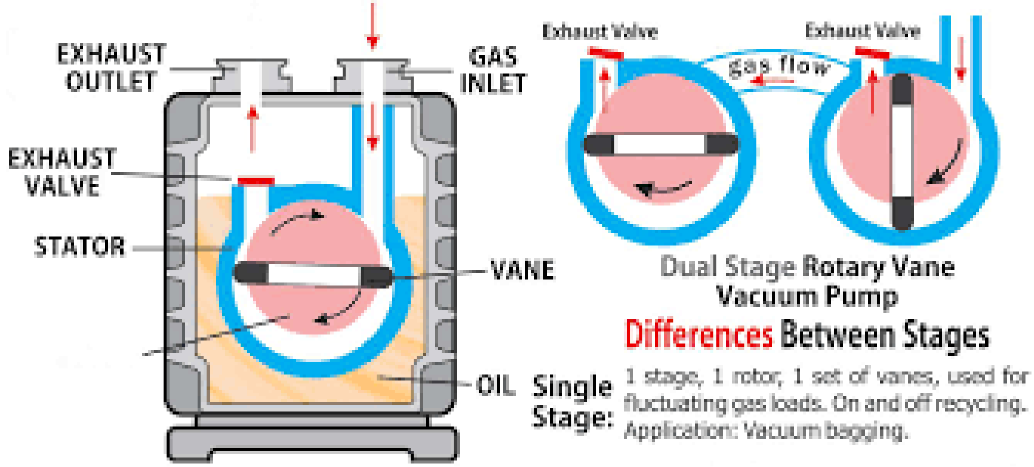

Rotary/scroll pump

10^{-1} Pa

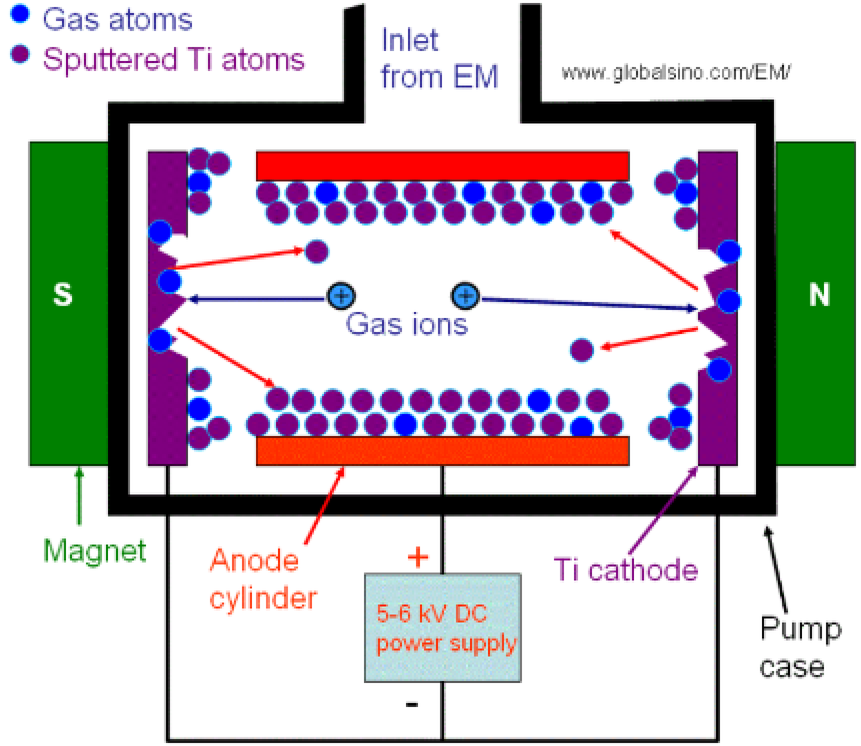

10^{-9} Pa

Ion pump

$10^{-2} – 10^{-9}$ Pa

Turbomolecular

Diffusion pumps

10^{-5} Pa

Electron sources

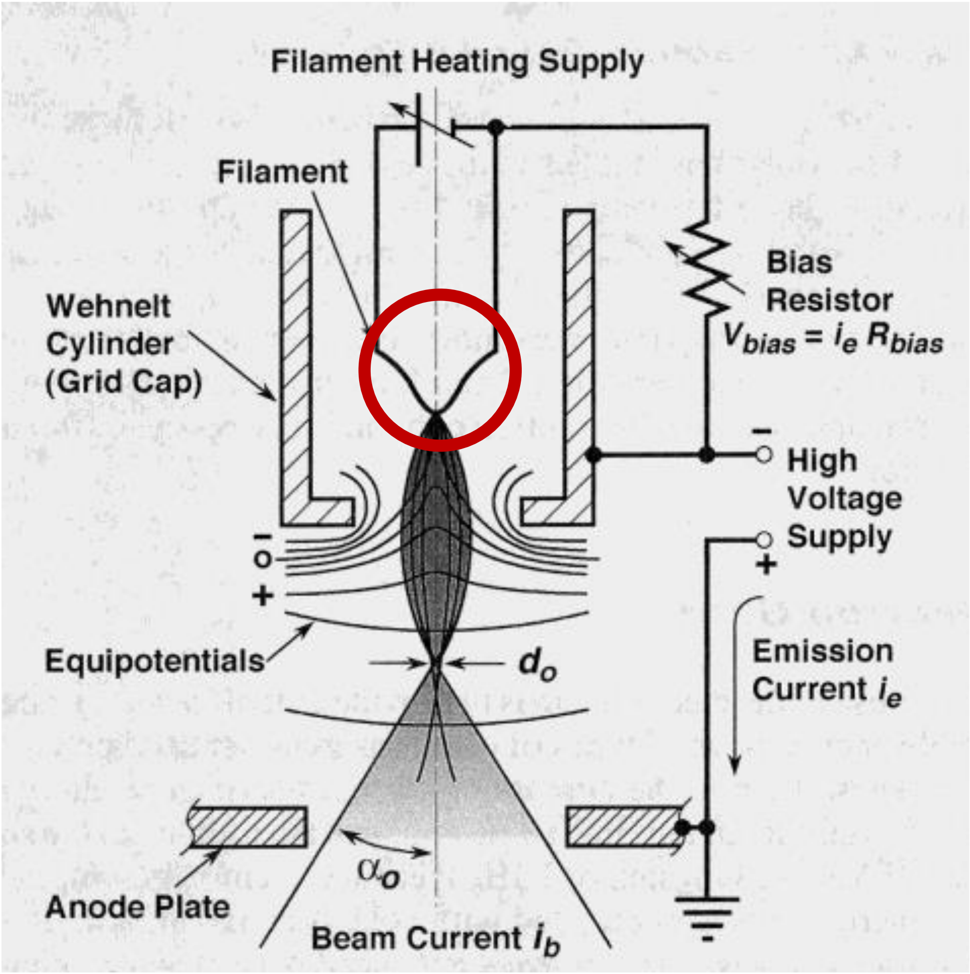

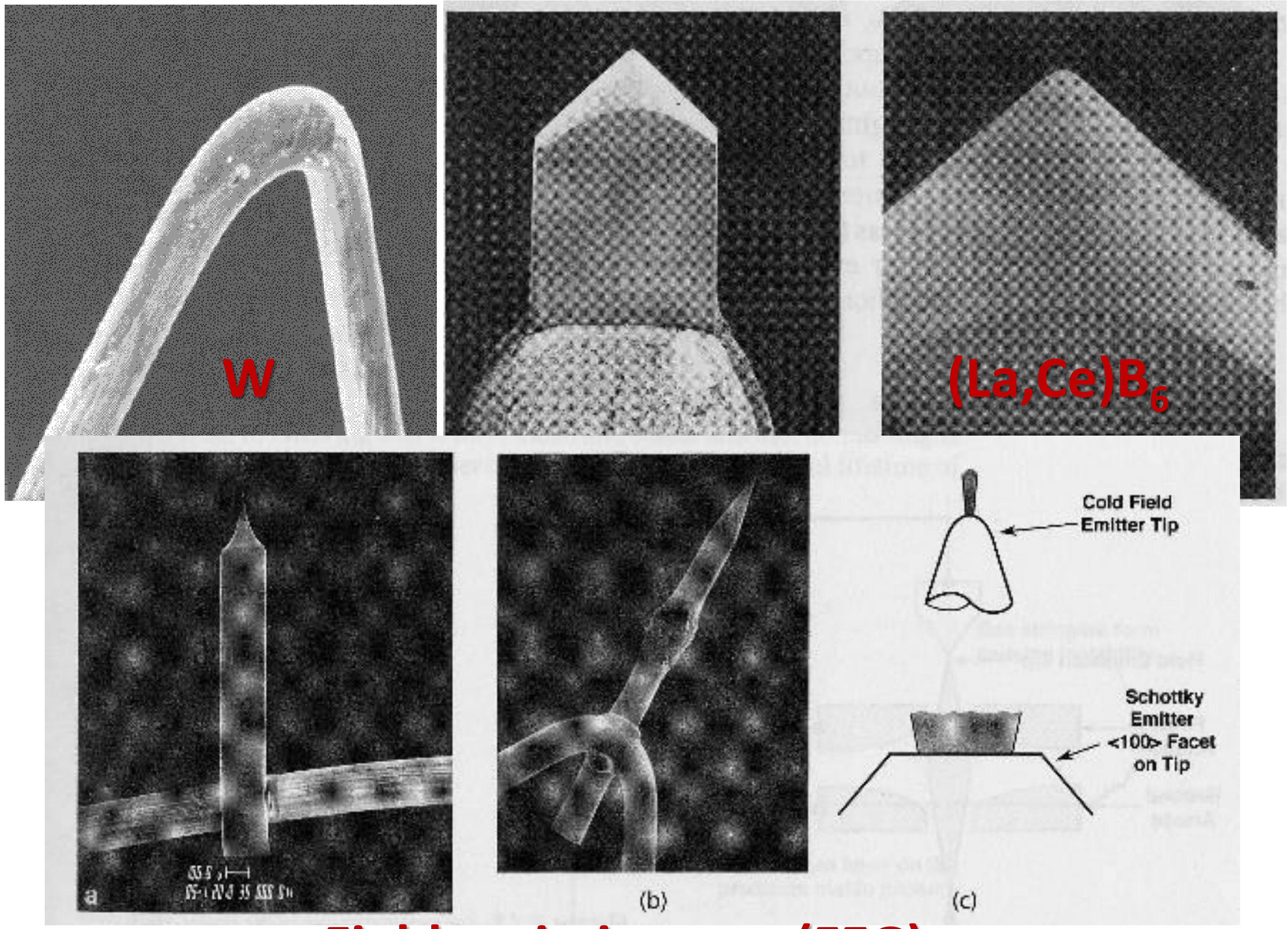

Field emission gun (FEG)
W wire + ZrO layer

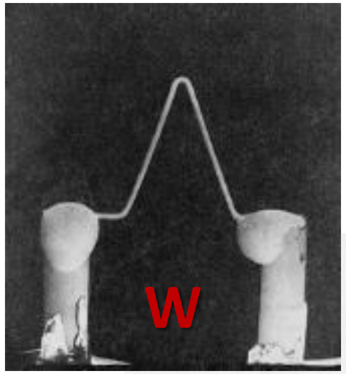

Electron sources

TABLE 5.1. Characteristics of the Three Principal Sources Operating at 100 kV

	Units	Tungsten	LaB_6	Field Emission
Work function, Φ	eV	4.5	2.4	4.5
Richardson's constant	A/m^2K^2	6×10^5	4×10^5	
Operating temperature	K	2700	1700	300
Current density	A/m^2	5×10^4	10^6	10^{10}
Crossover size	μm	50	10	<0.01
Brightness	A/m^2sr	10^9	5×10^{10}	10^{13}
Energy spread	eV	3	1.5	0.3
Emission current stability	%/hr	<1	<1	5
Vacuum	Pa	10^{-2}	10^{-4}	10^{-8}
Lifetime	hr	100	500	>1000

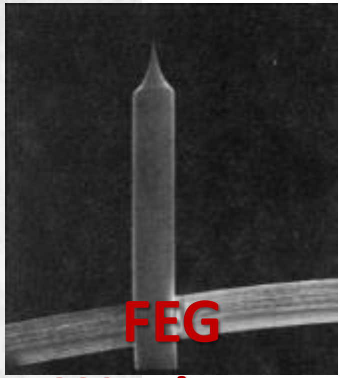

W wire + ZrO layer

Magnetic lenses

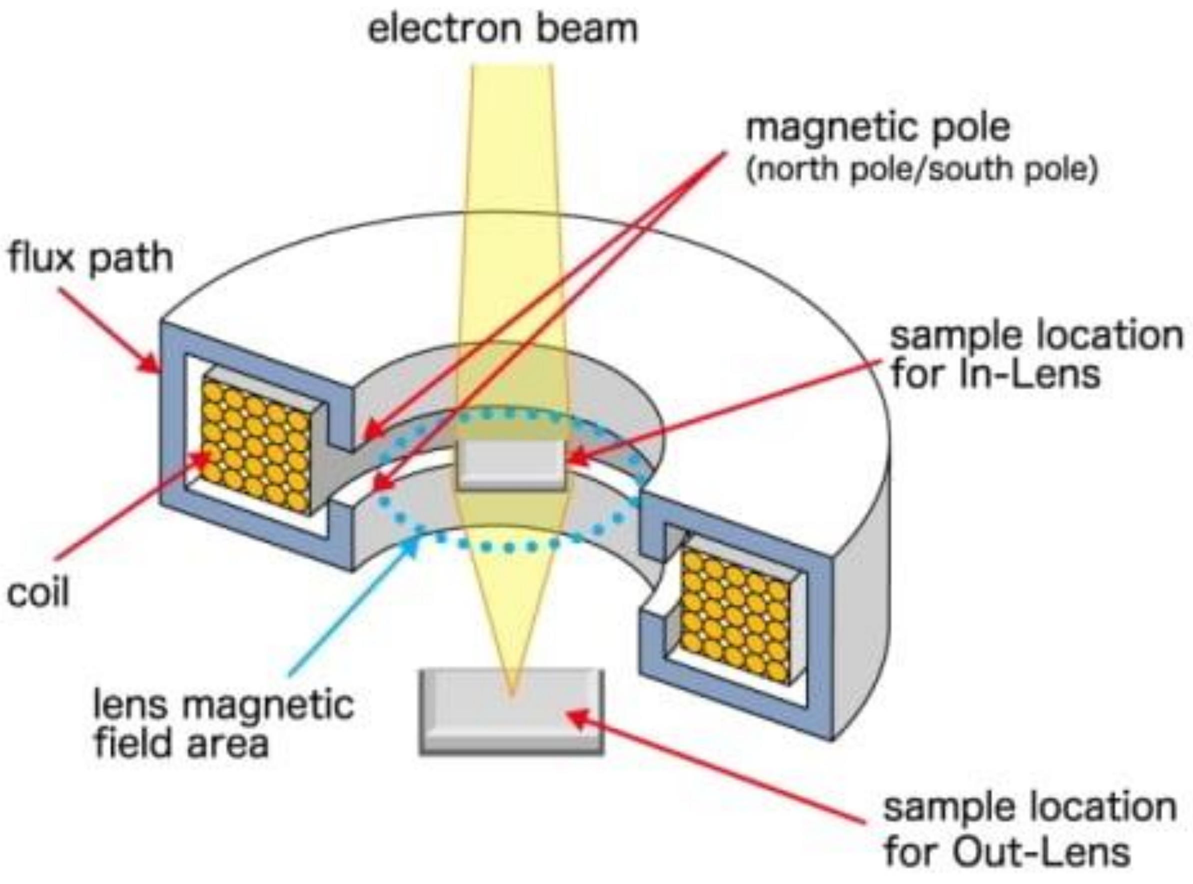

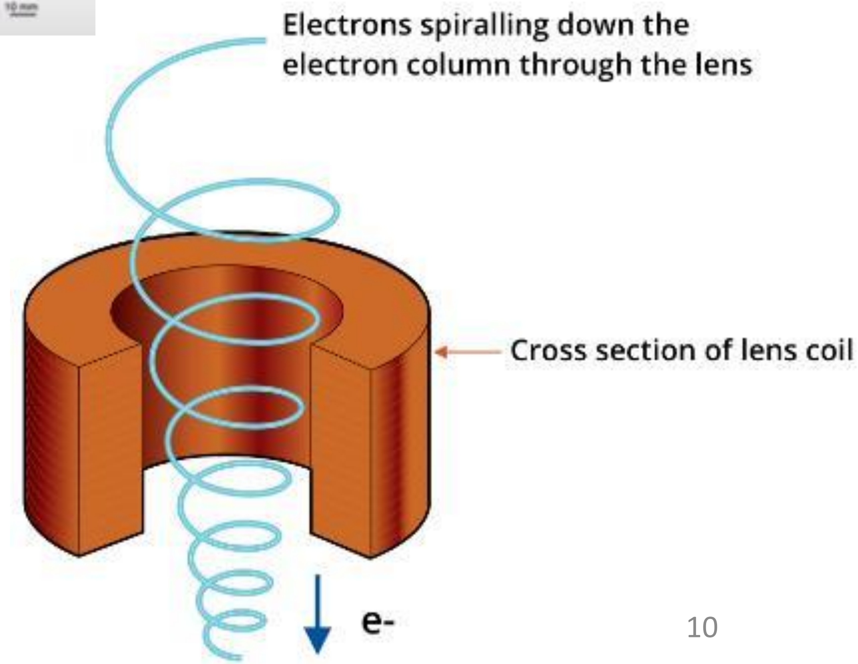

Magnetic lenses – expectation vs. reality

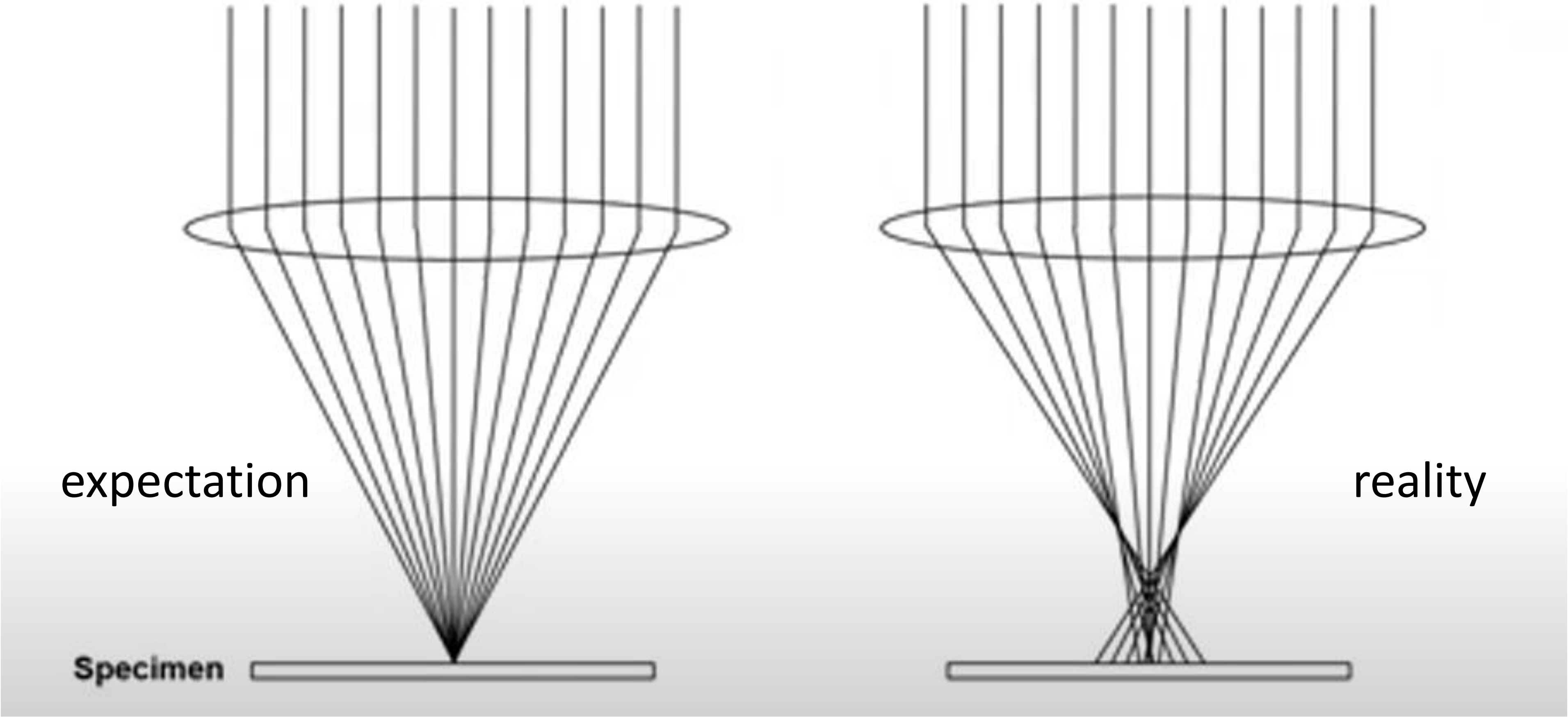

Abberations

Chromatic abberation

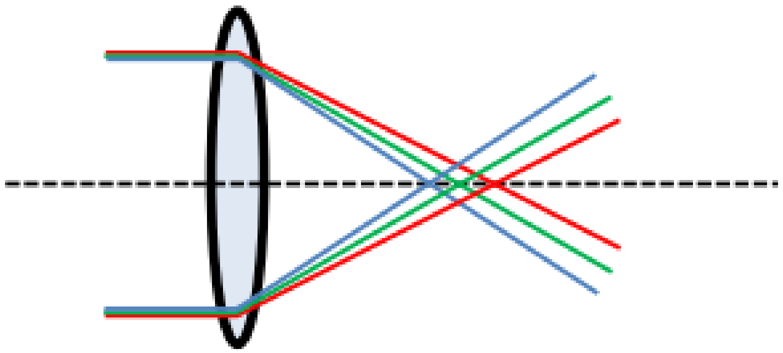

Spherical abberation

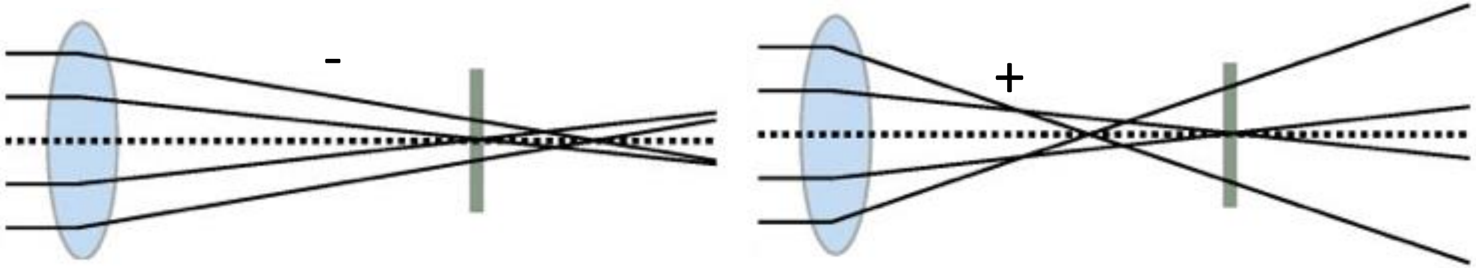

Astigmatism

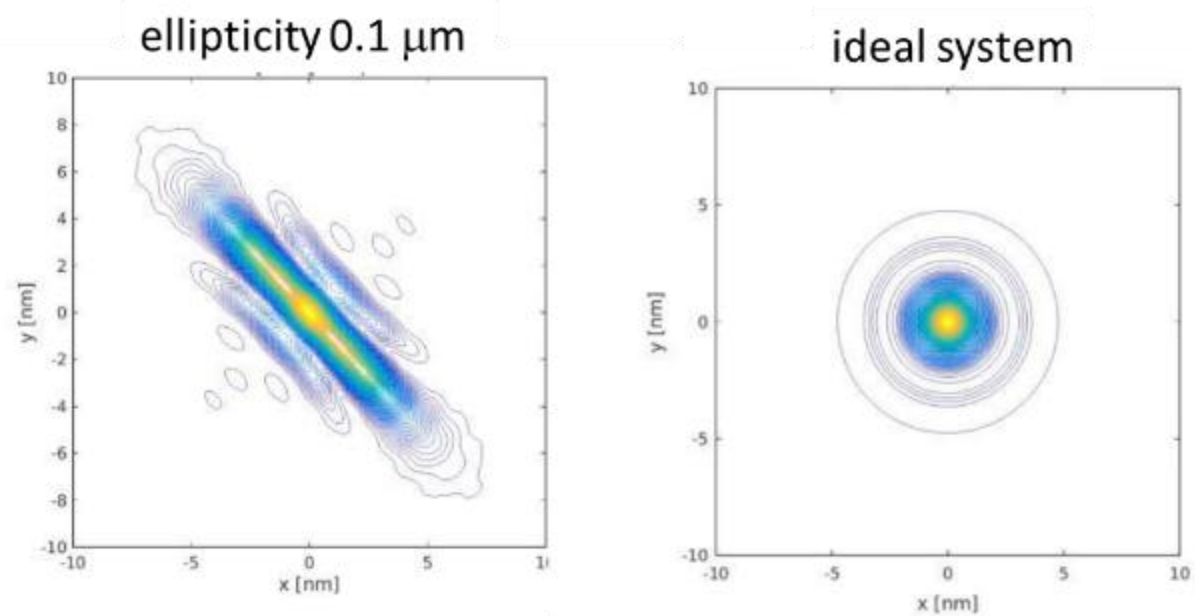

Coma abberation

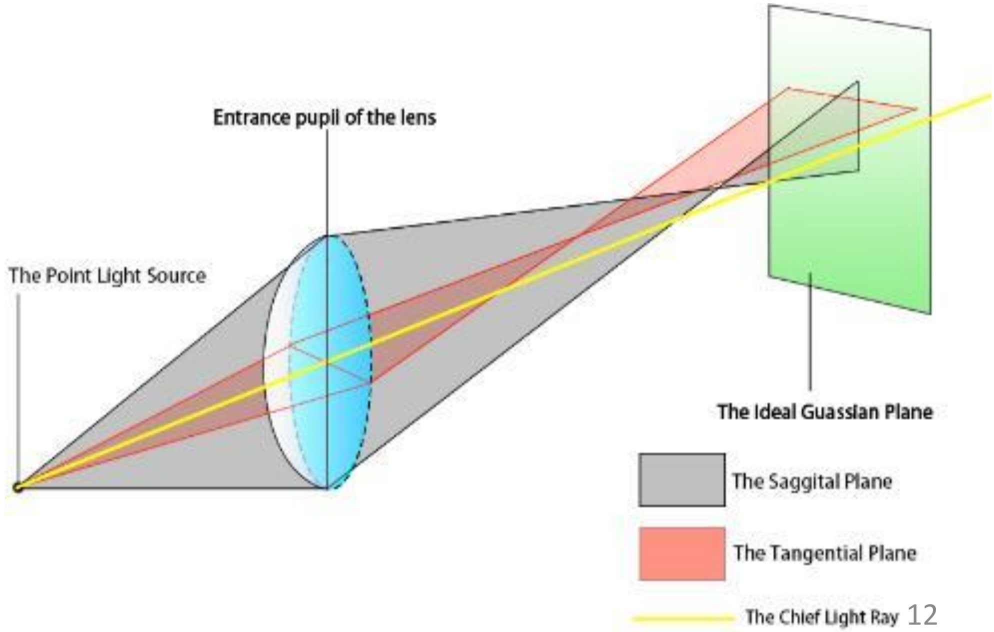

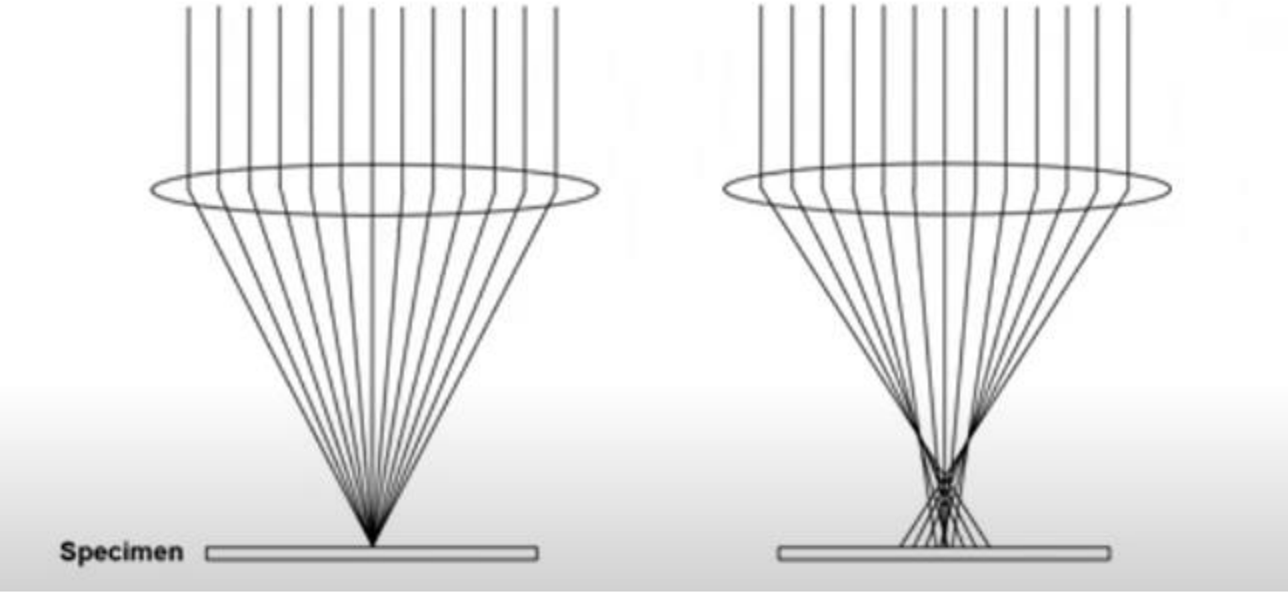

expectation reality

U=10kV (SEM) -> **λ = 0.01226 nm**

U=100kV (TEM) -> **λ = 0.0039 nm**

Visible light - > λ = 390 – 760 nm

Typical SEM -> d_d ~ **1 nm**

Typical TEM -> d_d ~ **0.1 nm**

High-end TEM (300 kV) -> d_d ~ **0.05 nm**

Interactions

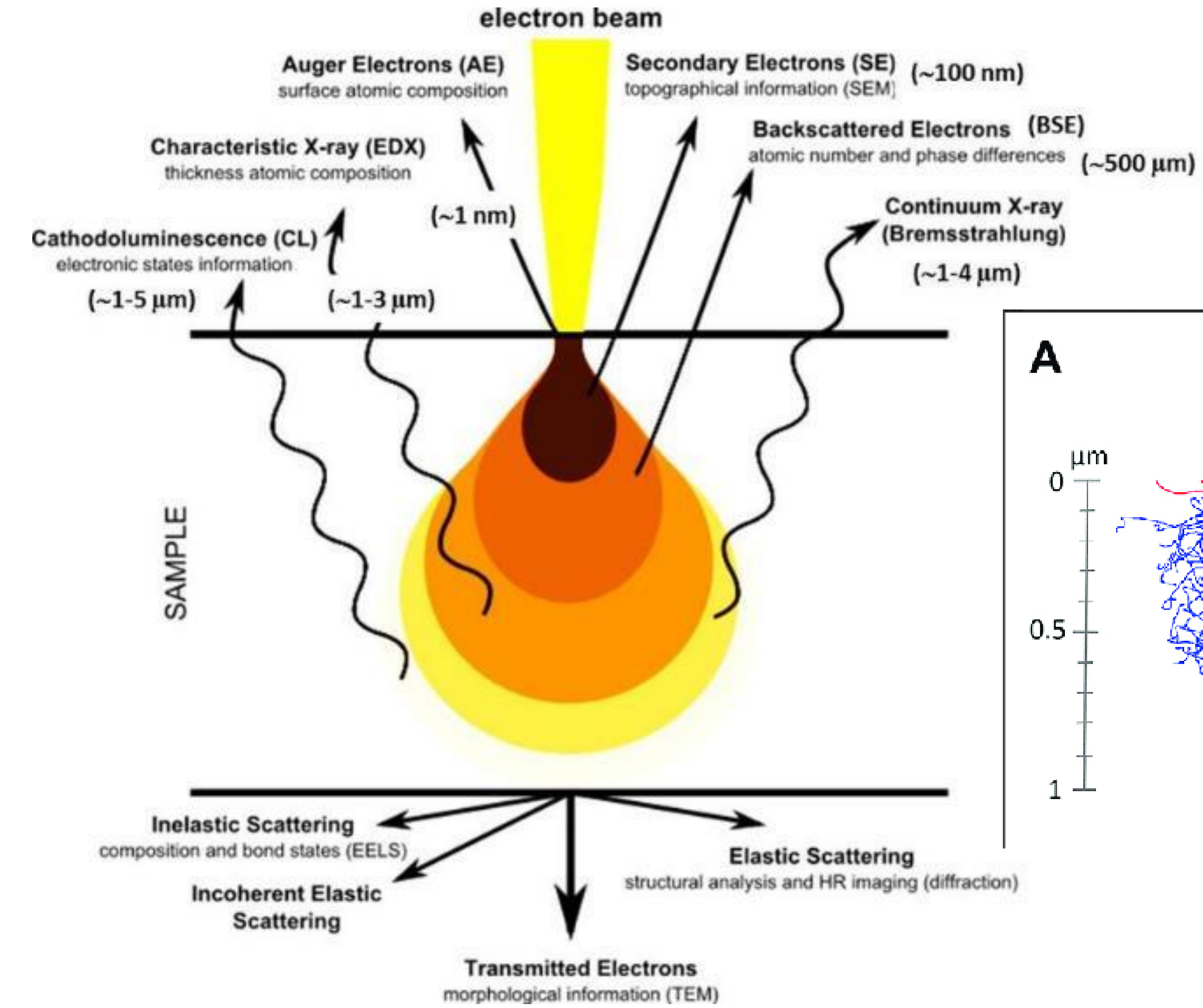

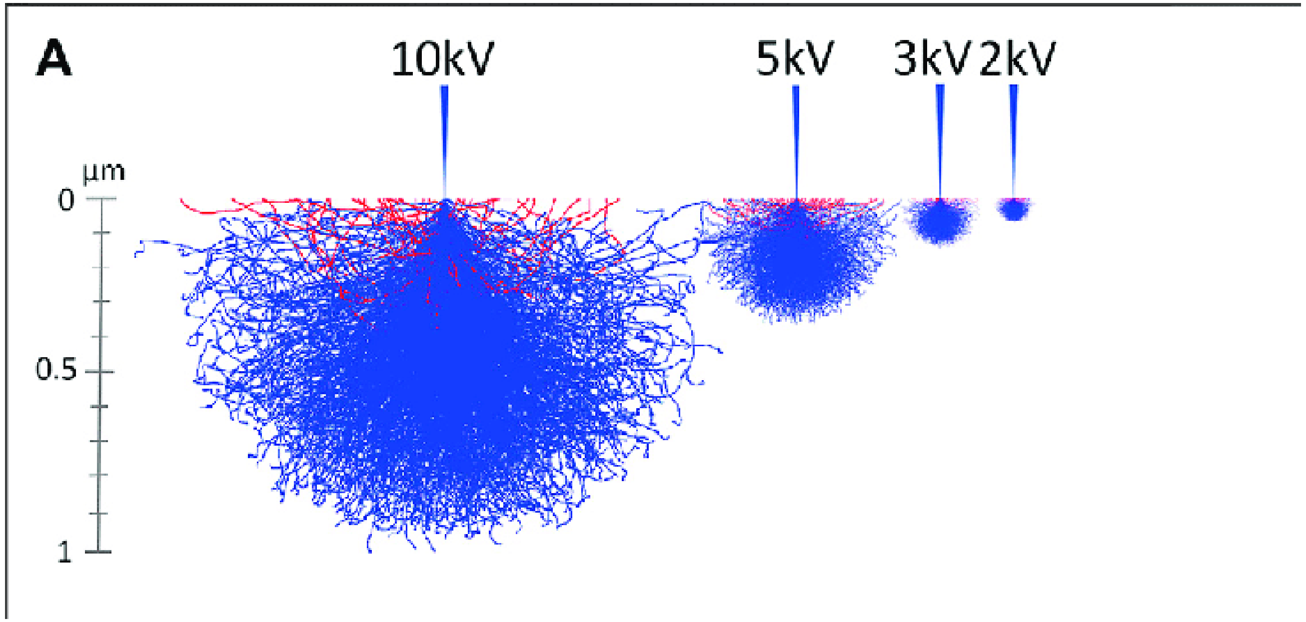

Interactions

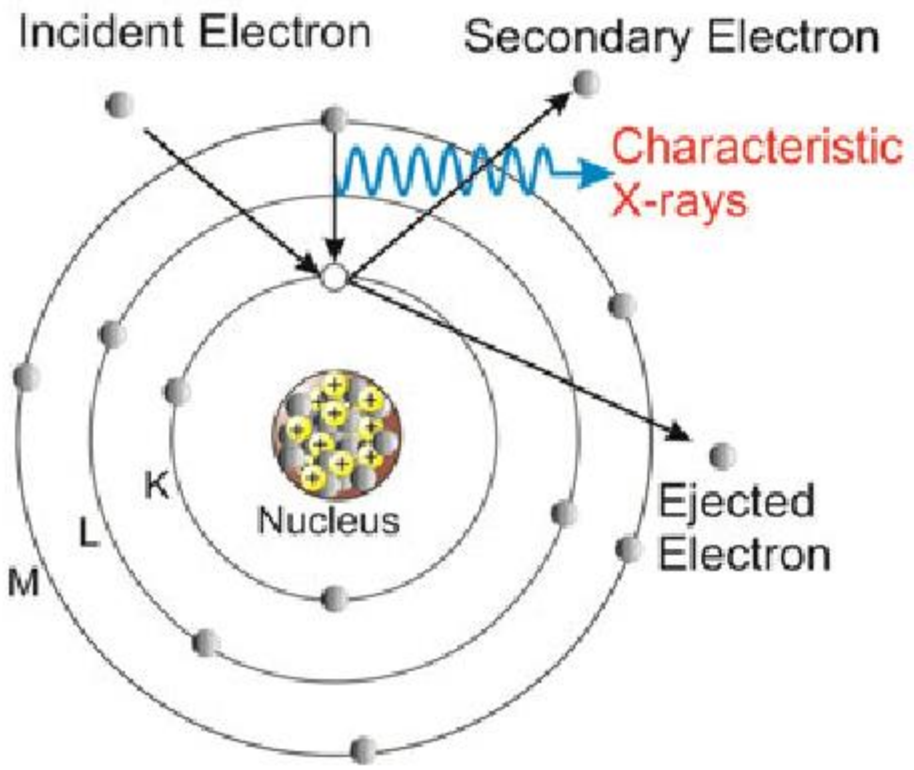

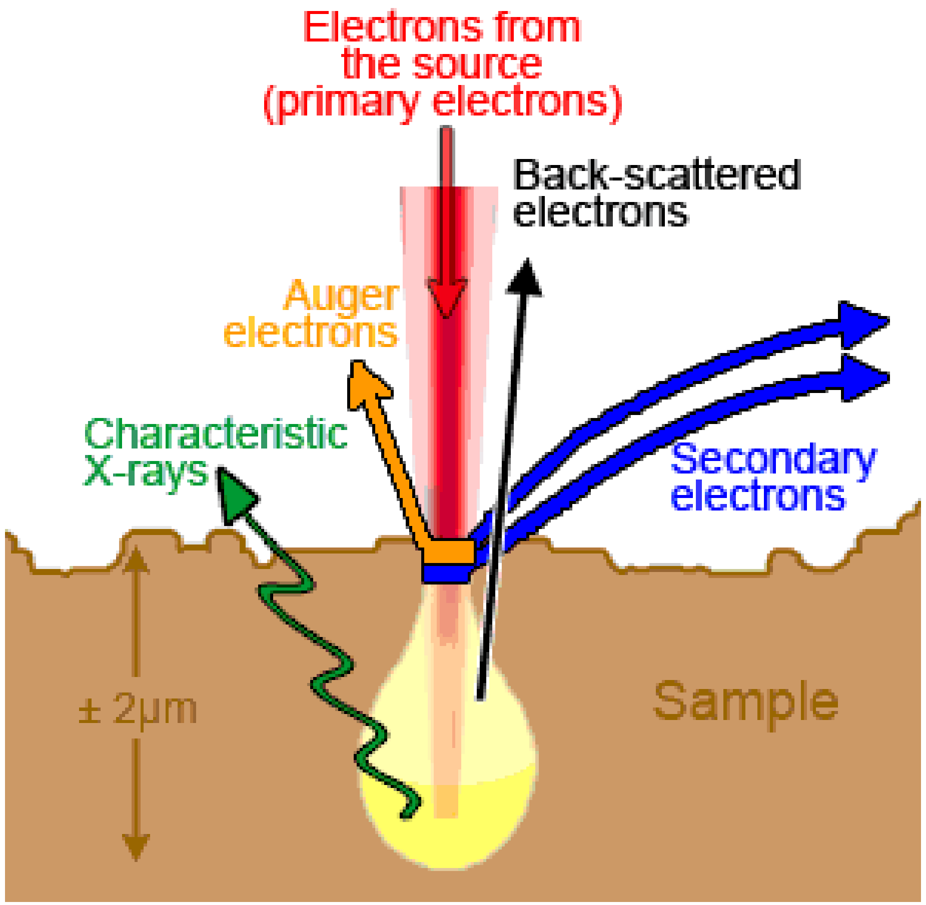

Primary

SE

BSE

Everhart-
Thornley SE

BSE

In – lens SE

BSE

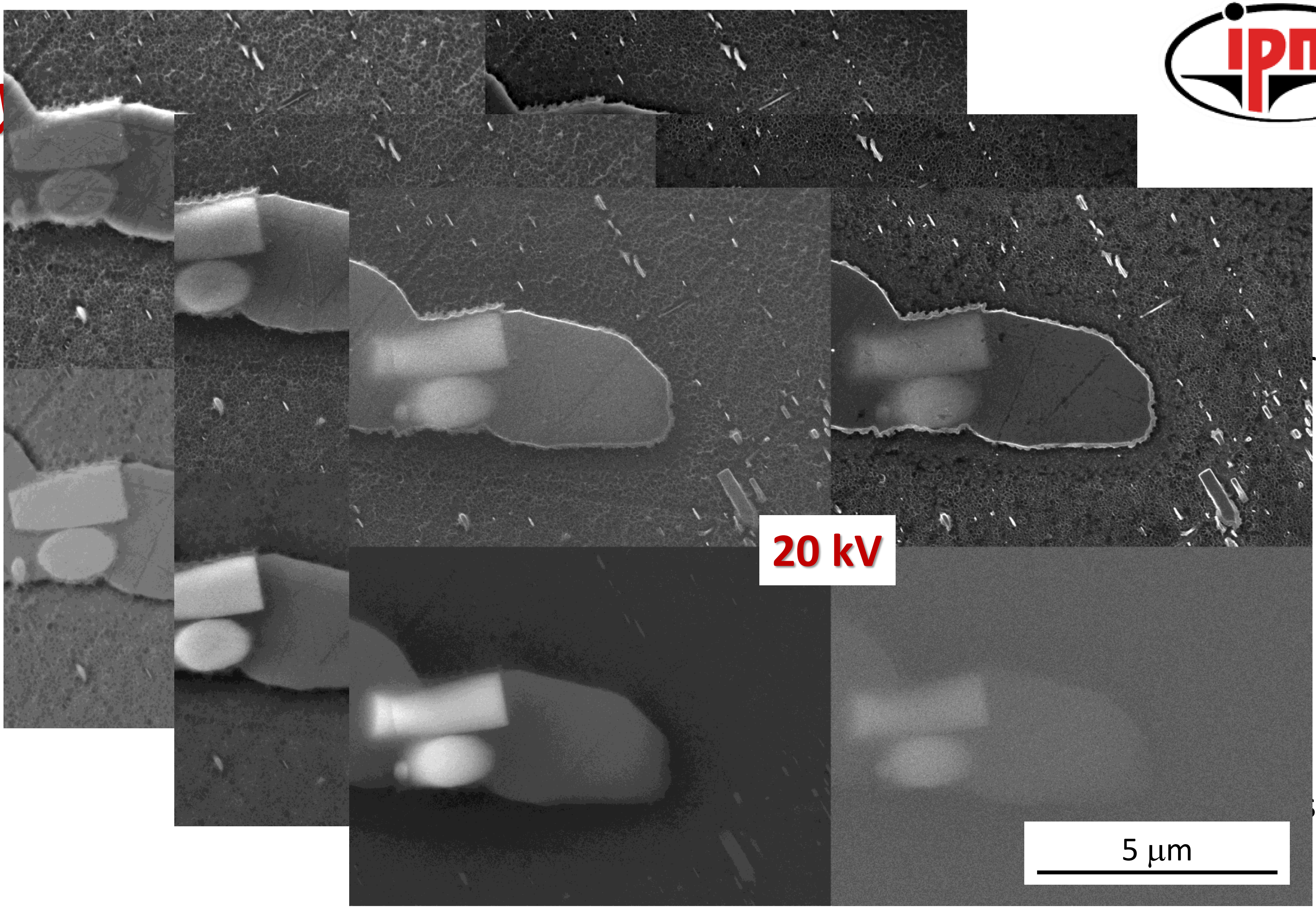

Secondary electrons

In – lens SE

Everhart-Thornley SE

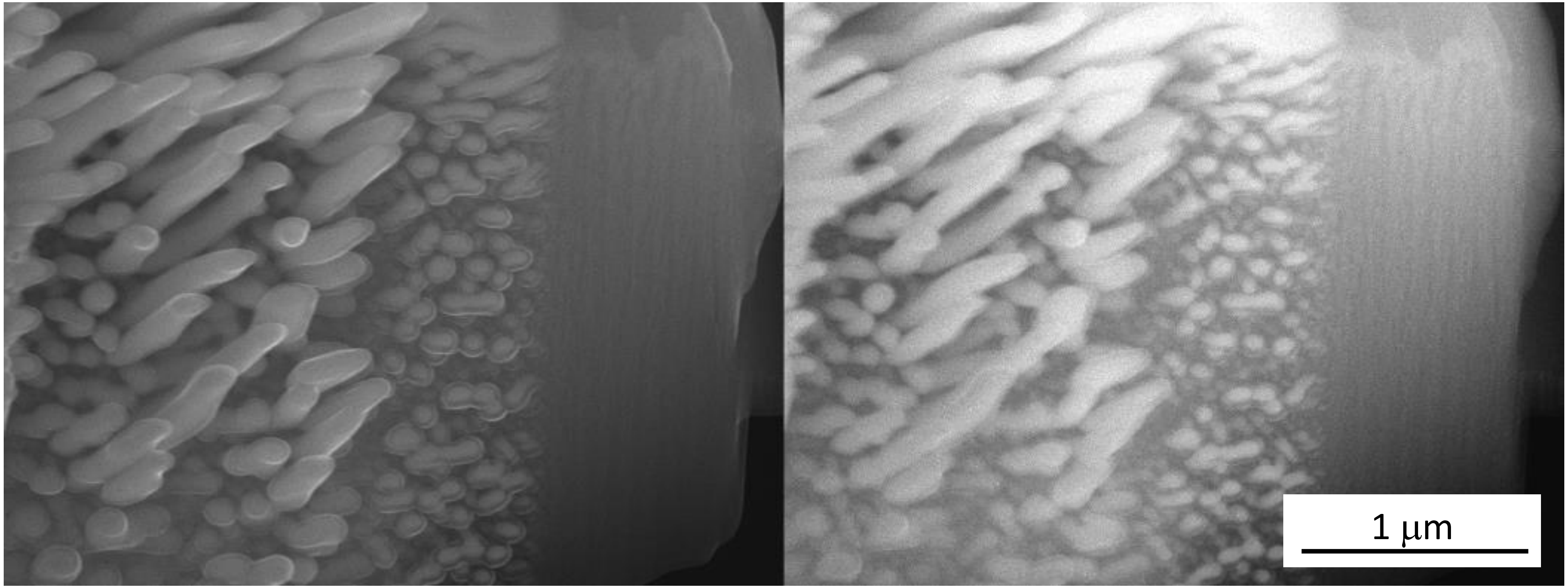

ECCI – Electron channeling contrast imagining

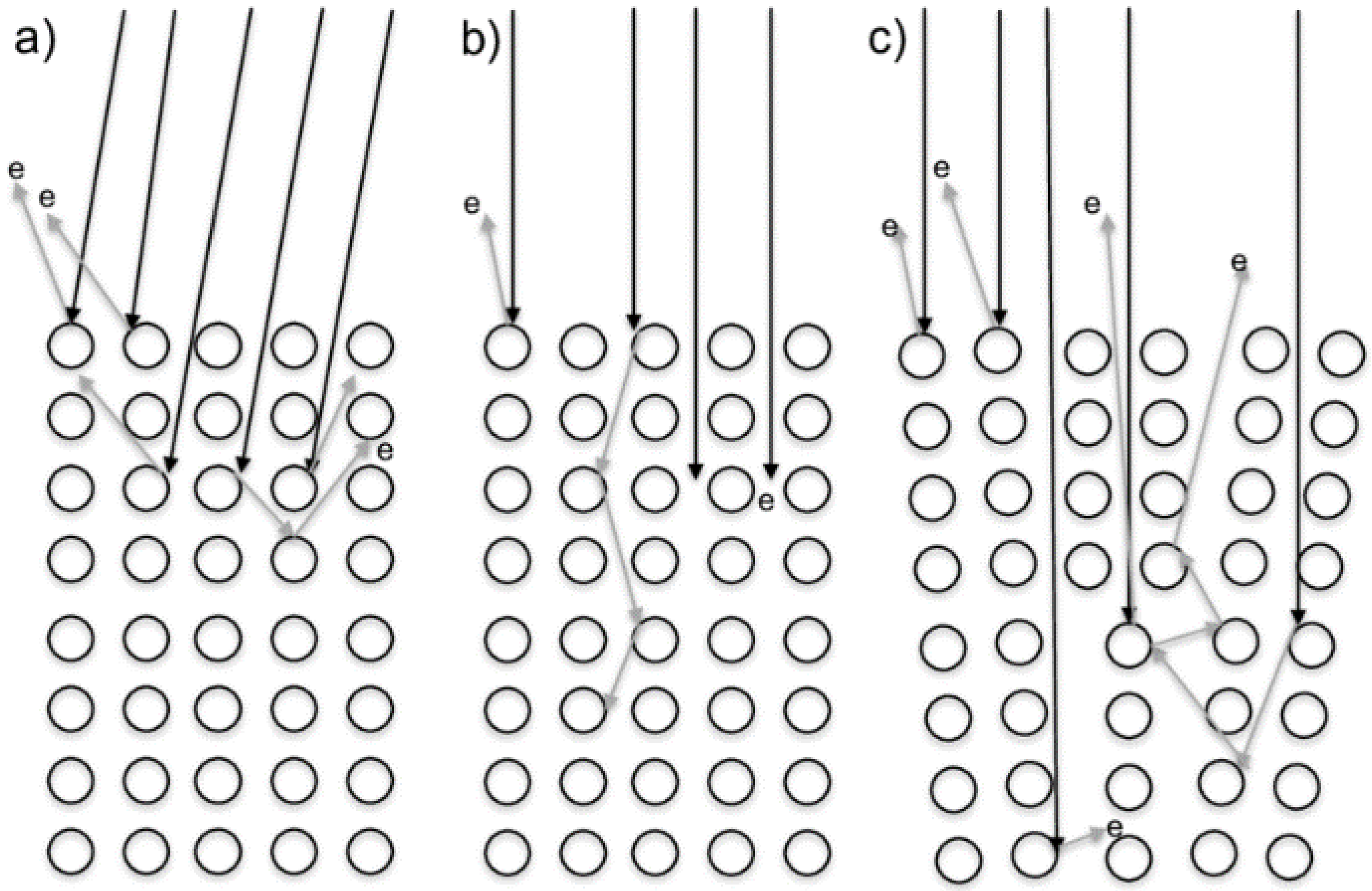

304L – after fatigue (specimen cross-cut)

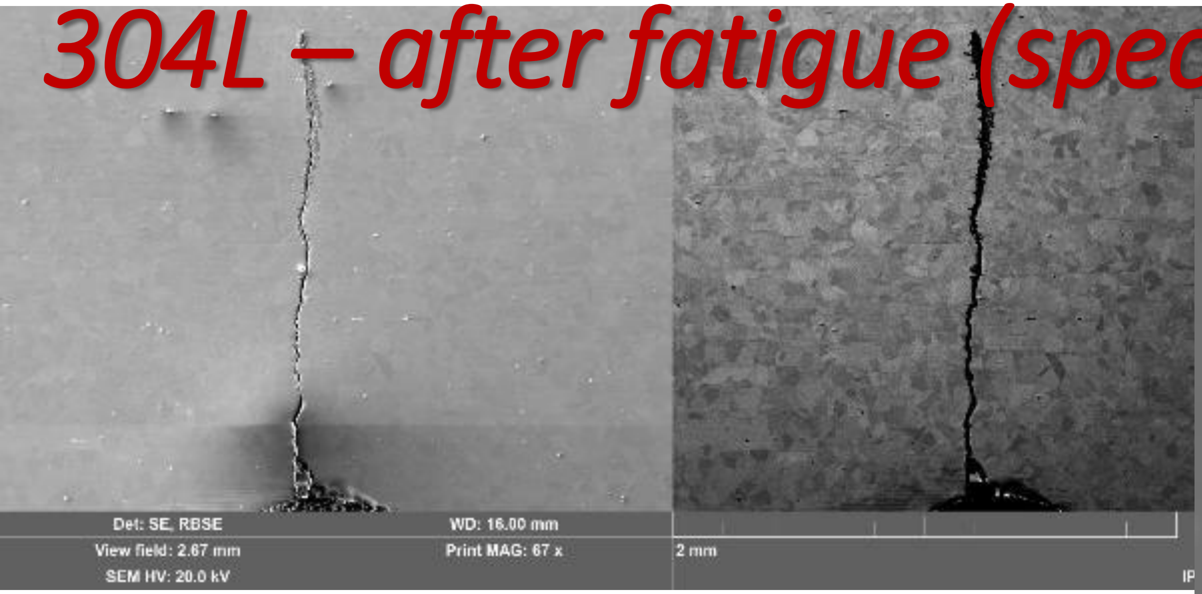

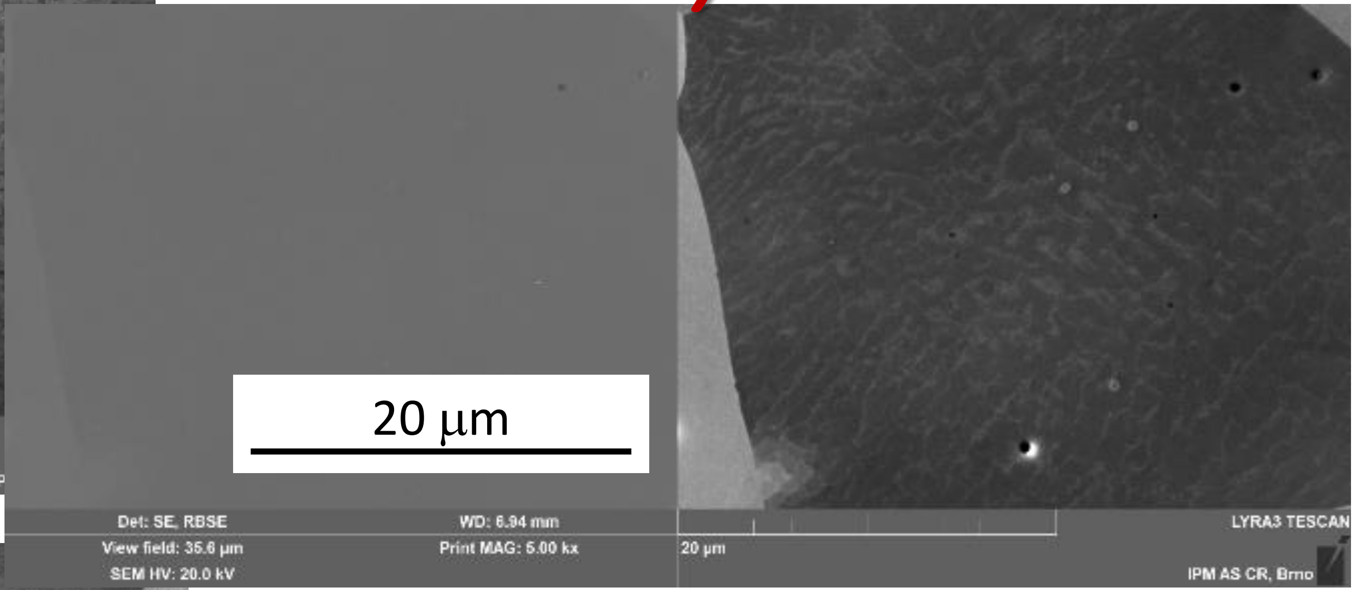

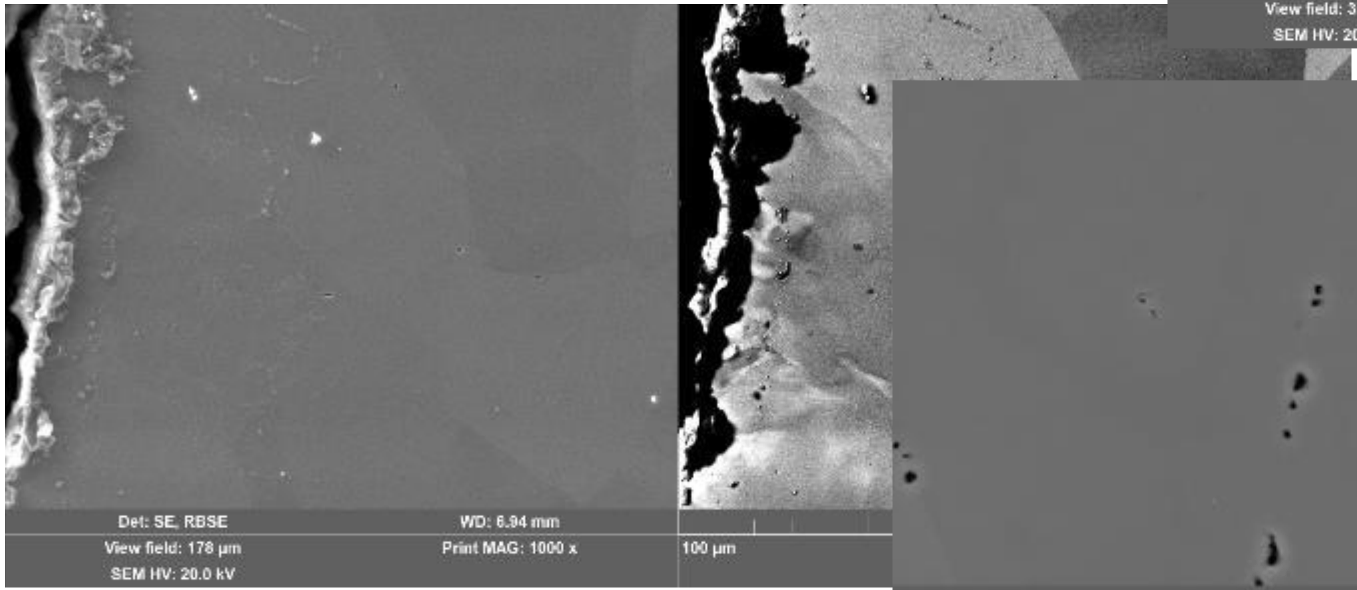

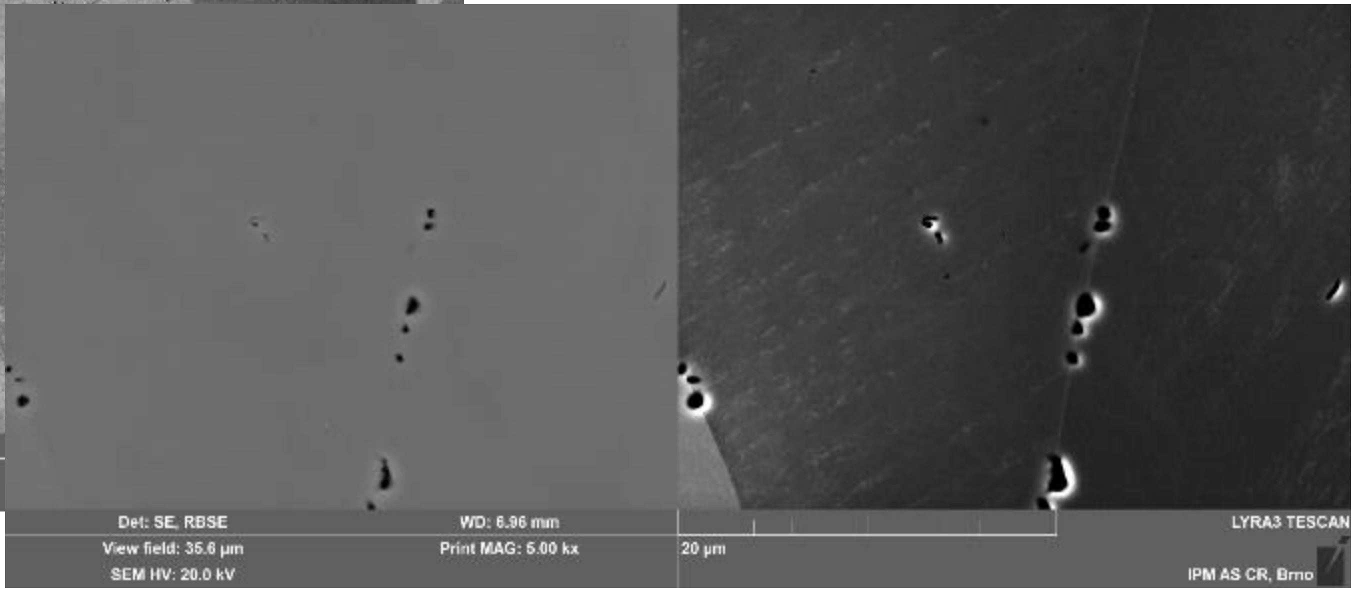

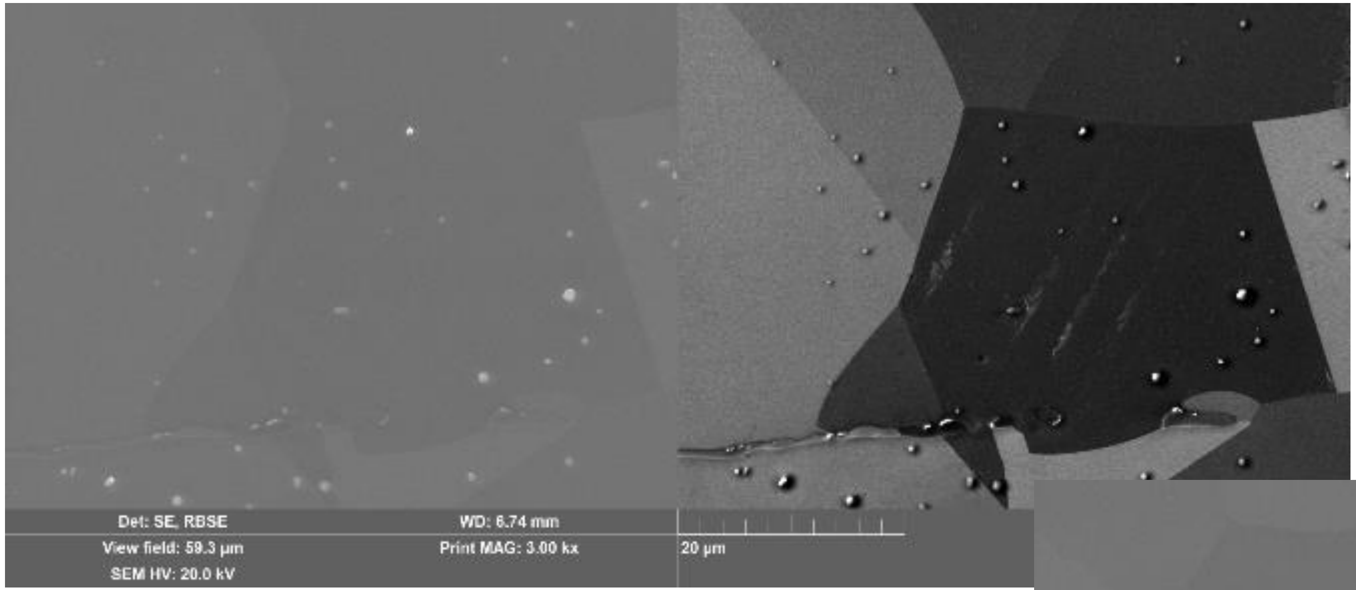
Det: SE, RBSE
WD: 6.74 mm
View field: 59.3 µm
Print MAG: 3.00 kx
20 µm
SEM HV: 20.0 kV

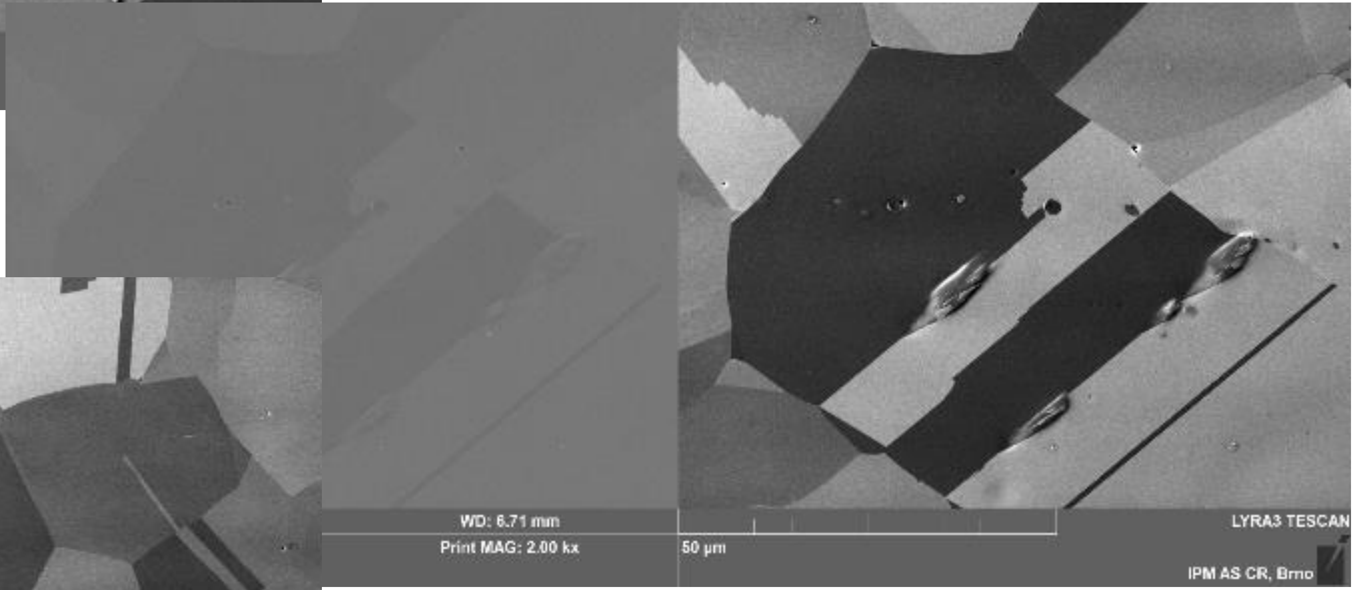
WD: 6.71 mm
Print MAG: 2.00 kx
50 µm
LYRA3 TESCAN
IPM AS CR, Brno

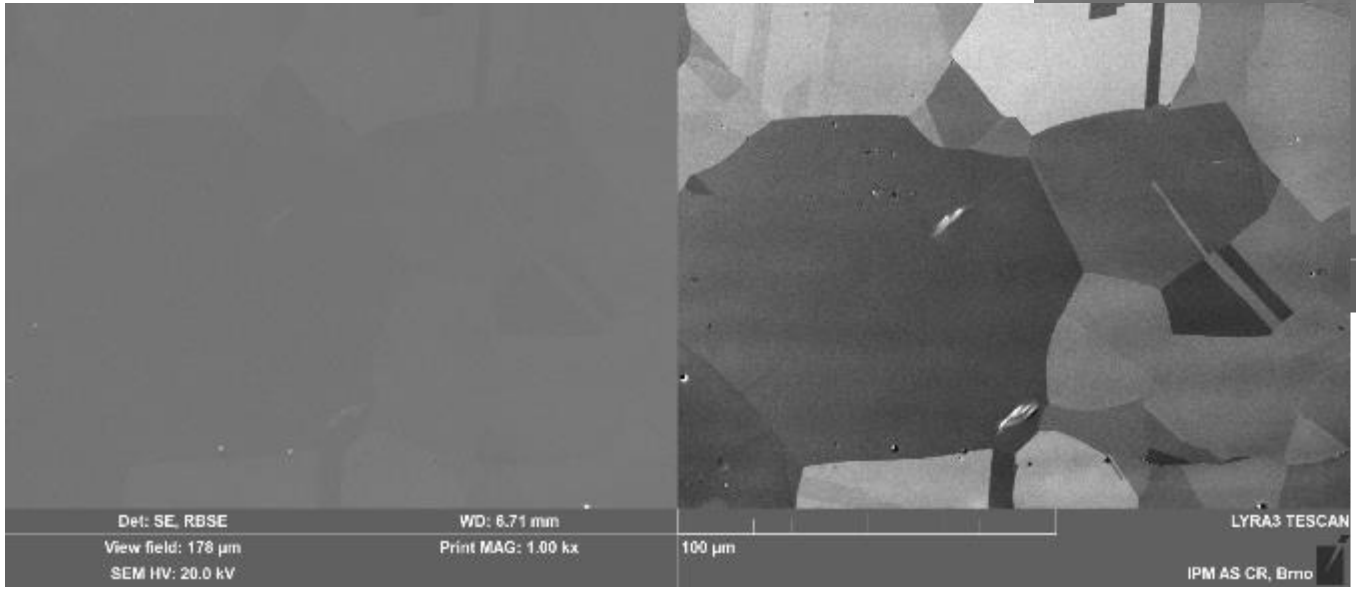
Det: SE, RBSE
WD: 6.71 mm
View field: 178 µm
Print MAG: 1.00 kx
100 µm
SEM HV: 20.0 kV
LYRA3 TESCAN
IPM AS CR, Brno

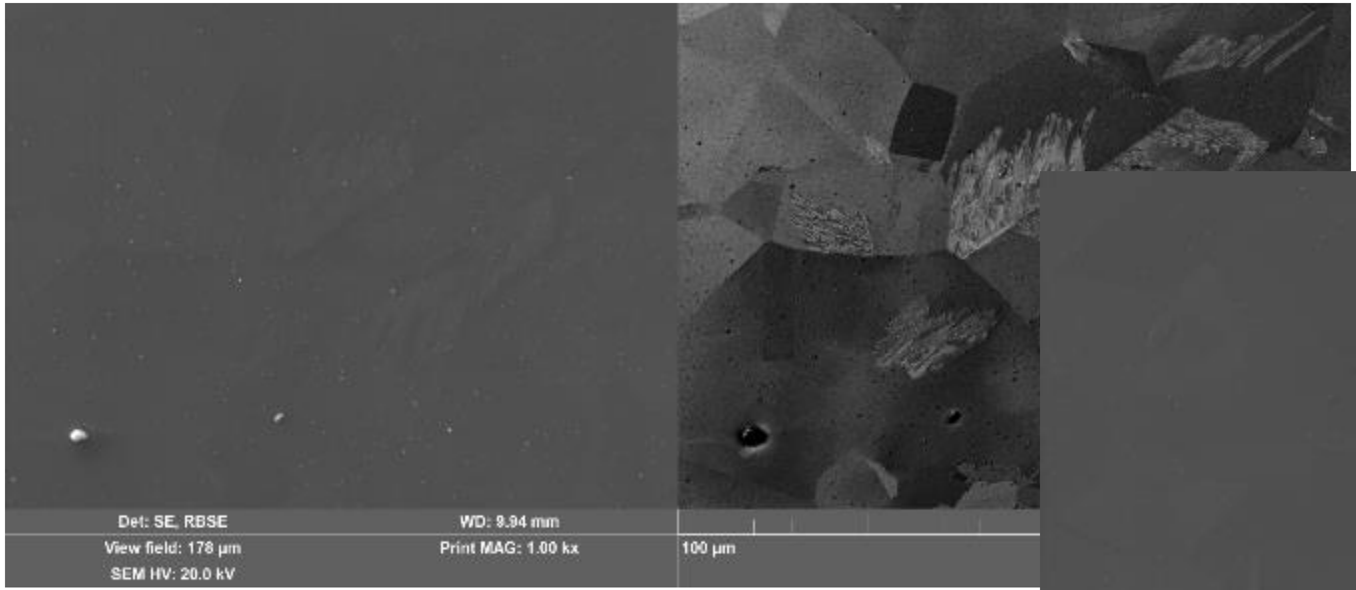
Det: SE, RBSE
WD: 9.94 mm
View field: 178 µm
Print MAG: 1.00 kx
SEM HV: 20.0 kV
100 µm

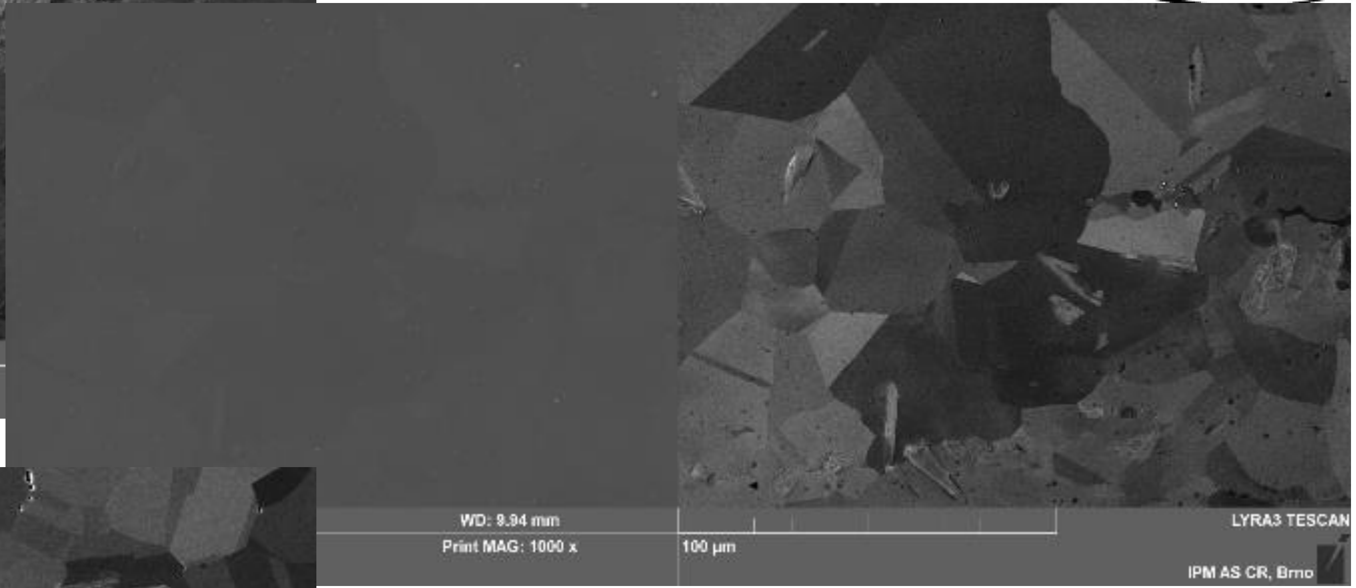
WD: 9.94 mm
Print MAG: 1000 x
100 µm
LYRA3 TESCAN
IPM AS CR, Brno

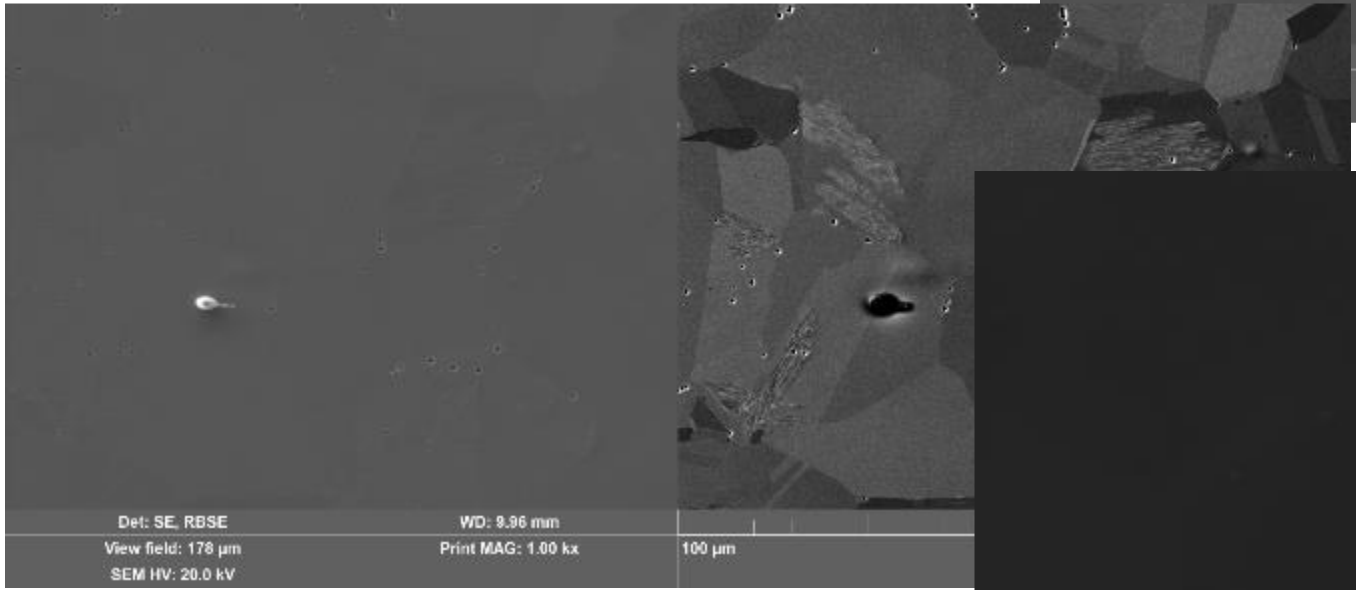
Det: SE, RBSE
WD: 9.96 mm
View field: 178 µm
Print MAG: 1.00 kx
SEM HV: 20.0 kV
100 µm

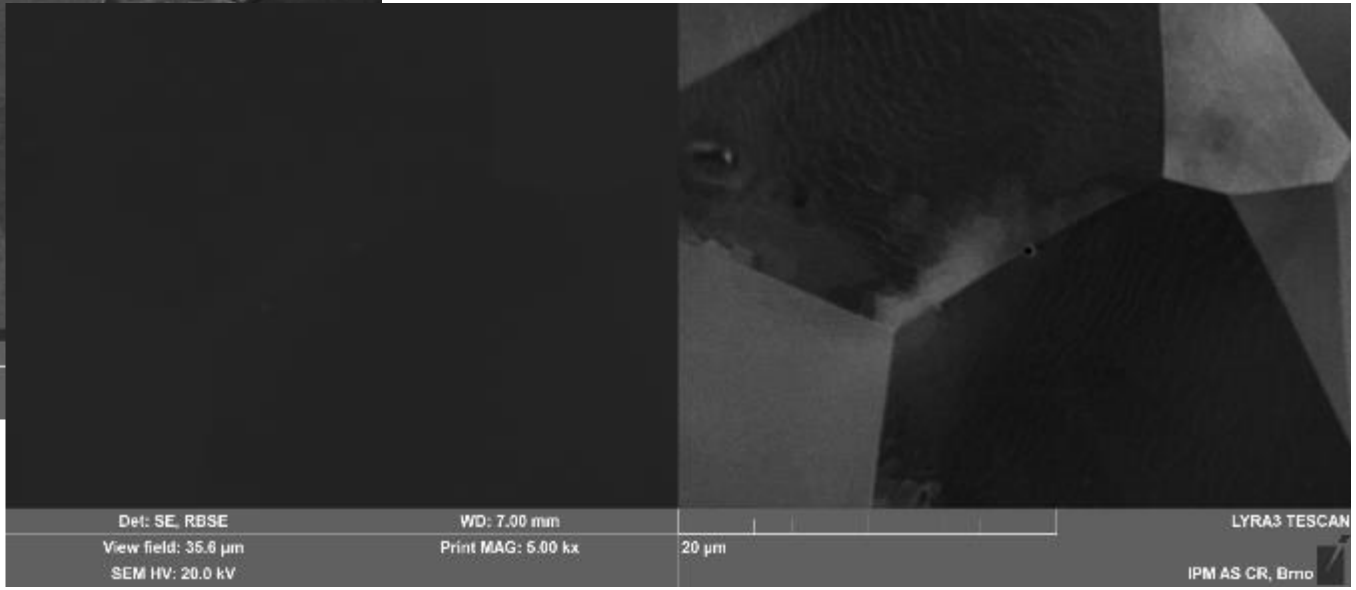
Det: SE, RBSE
WD: 7.00 mm
View field: 35.6 µm
Print MAG: 5.00 kx
SEM HV: 20.0 kV
20 µm
LYRA3 TESCAN
IPM AS CR, Brno

Energy and wave dispersive spectroscopy

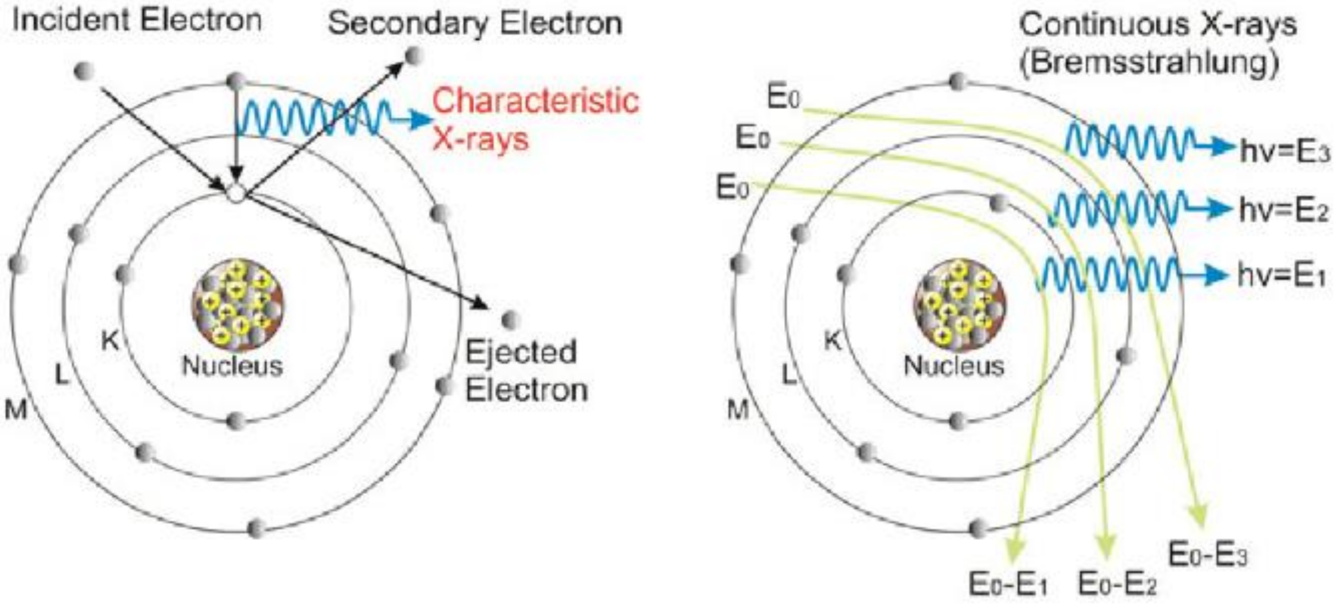

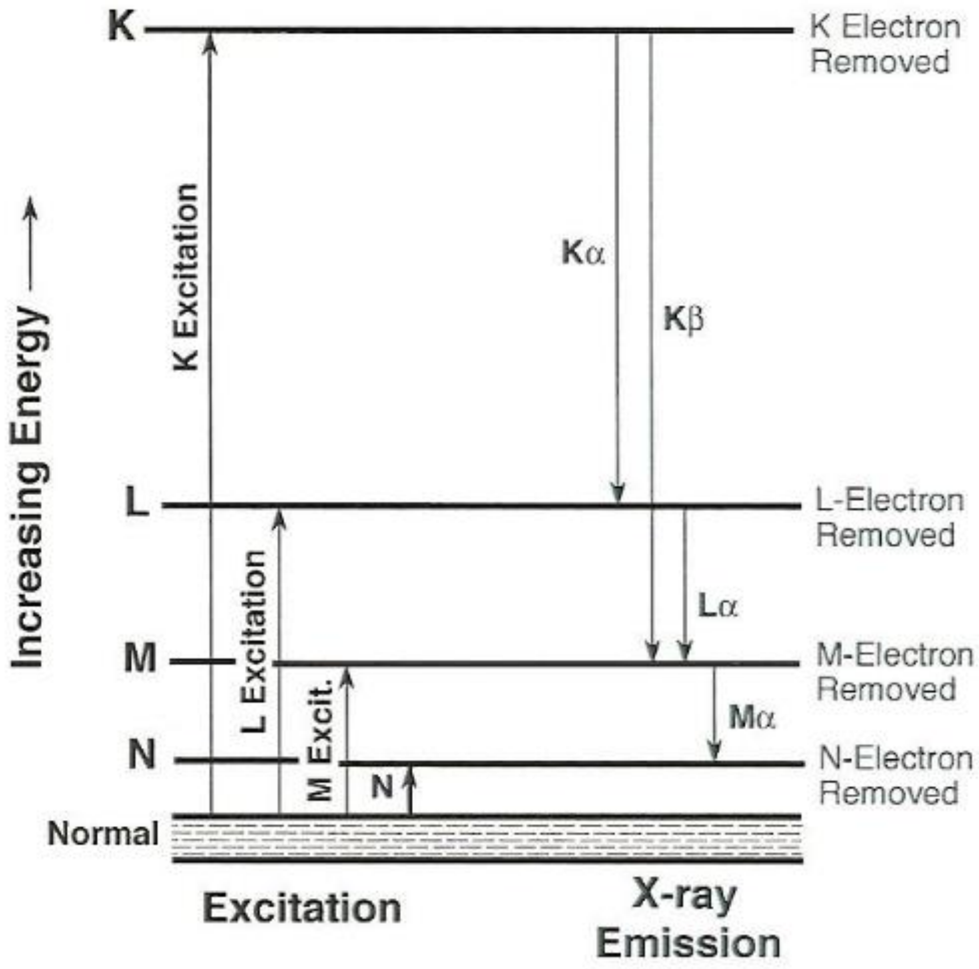

Energy dispersive spectroscopy - EDS

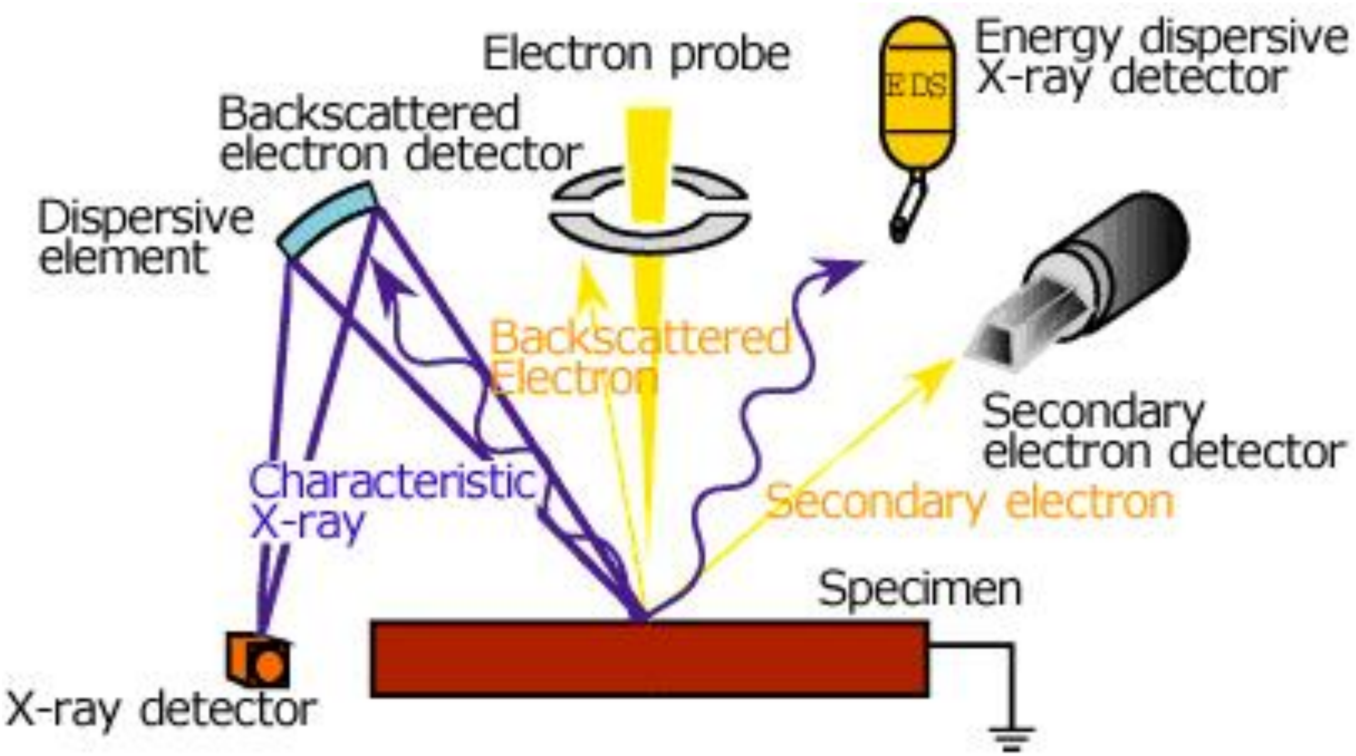

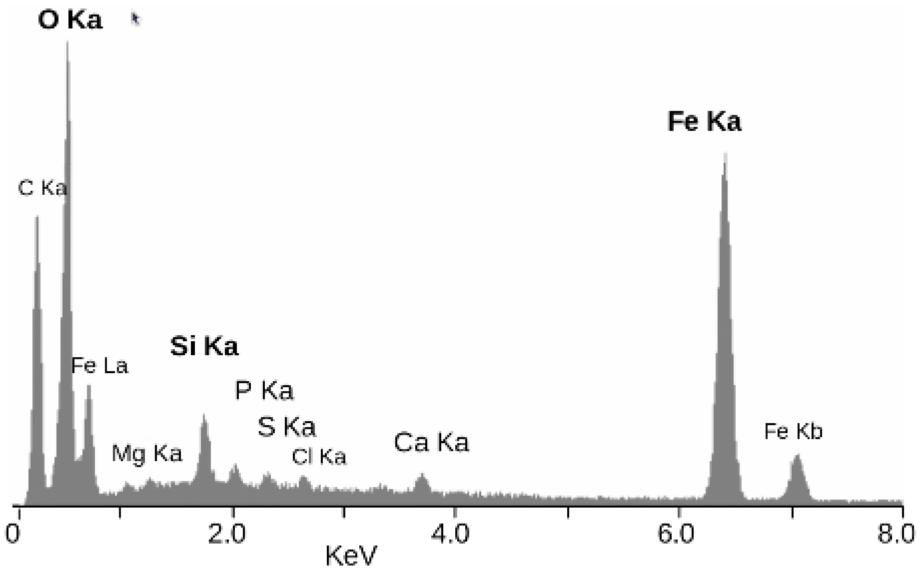

Wave dispersive spectroscopy - WDS

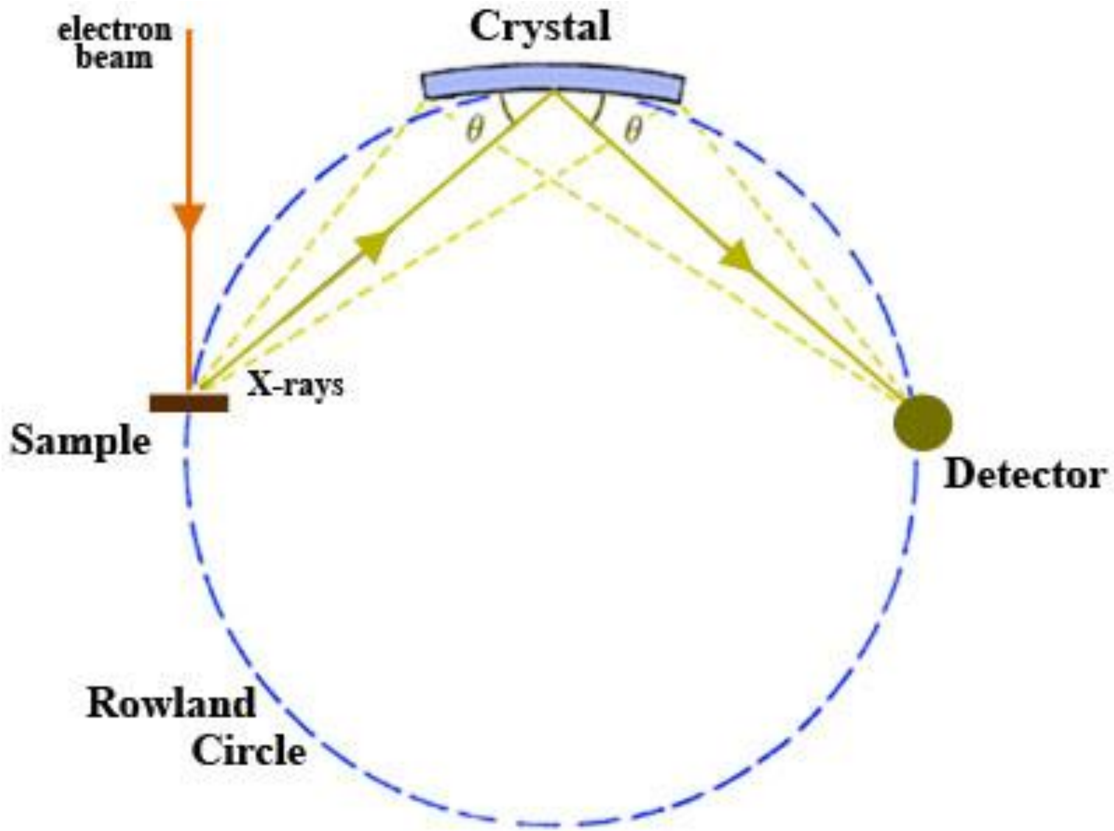

$$2d \sin \theta = n.\lambda$$

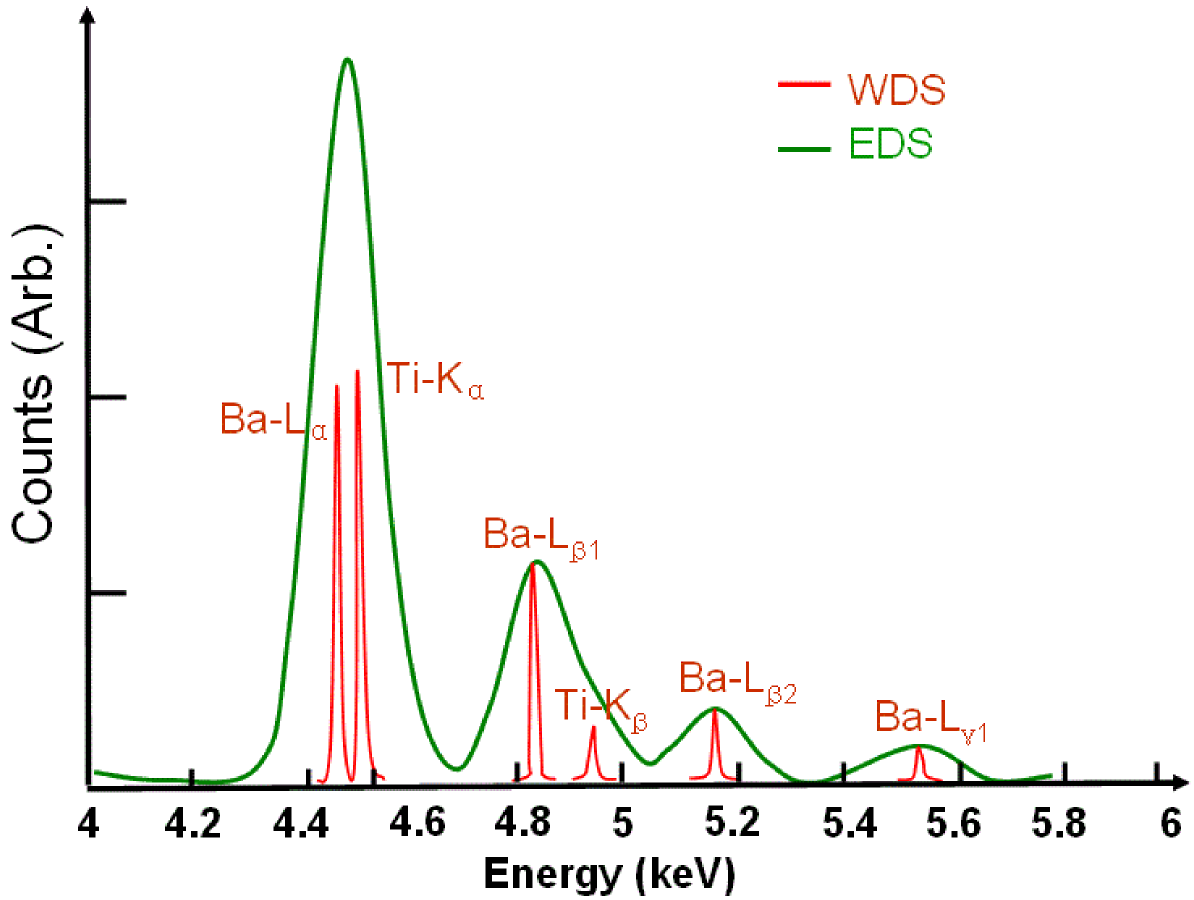

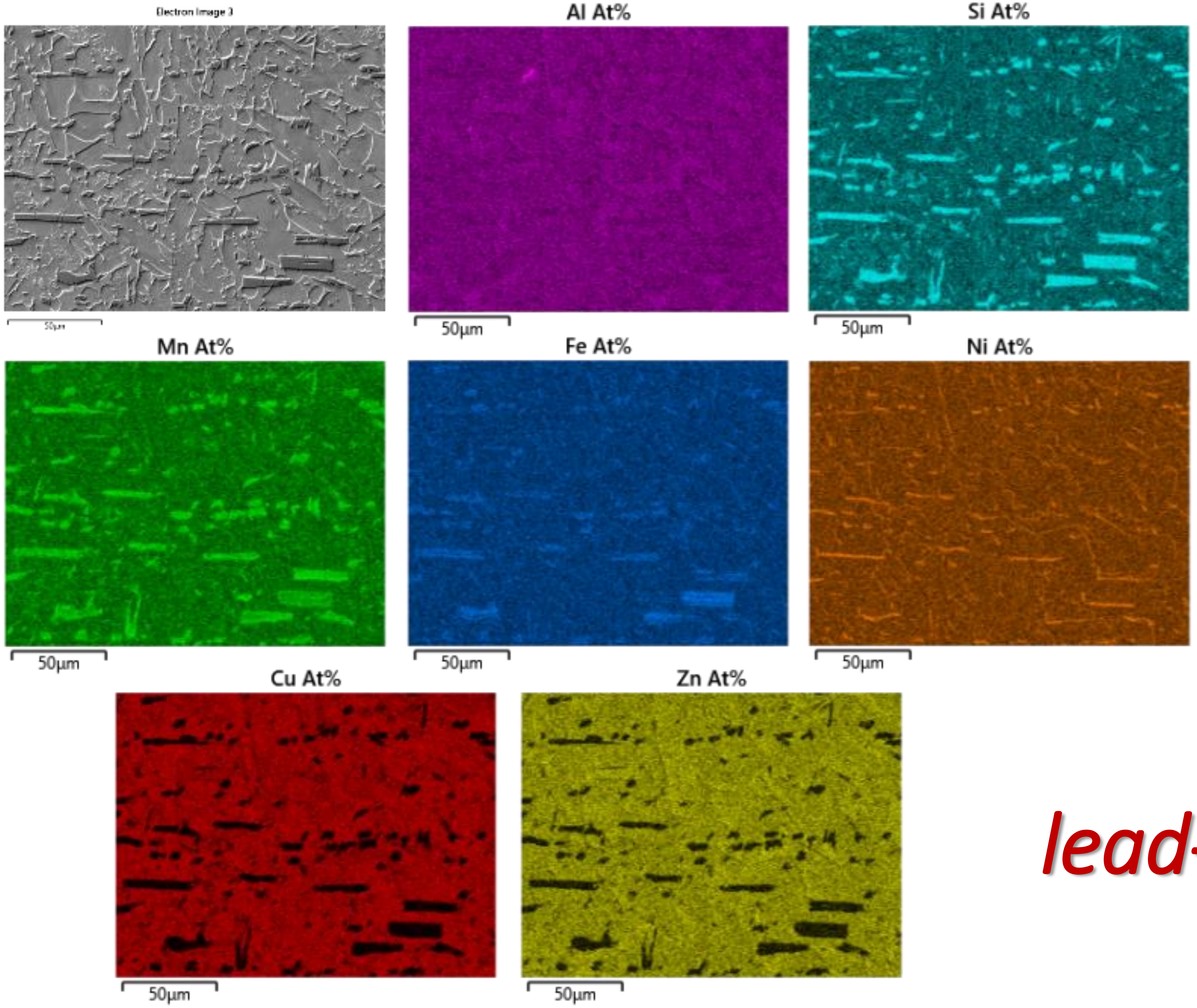

element	wt. %
Cu	60.1
Zn	27.5
Mn	6.5
Si	2.6
Al	1.3
Ni	1.1
Fe	1.0

lead-free brass

Electron backscattered diffraction - EBSD

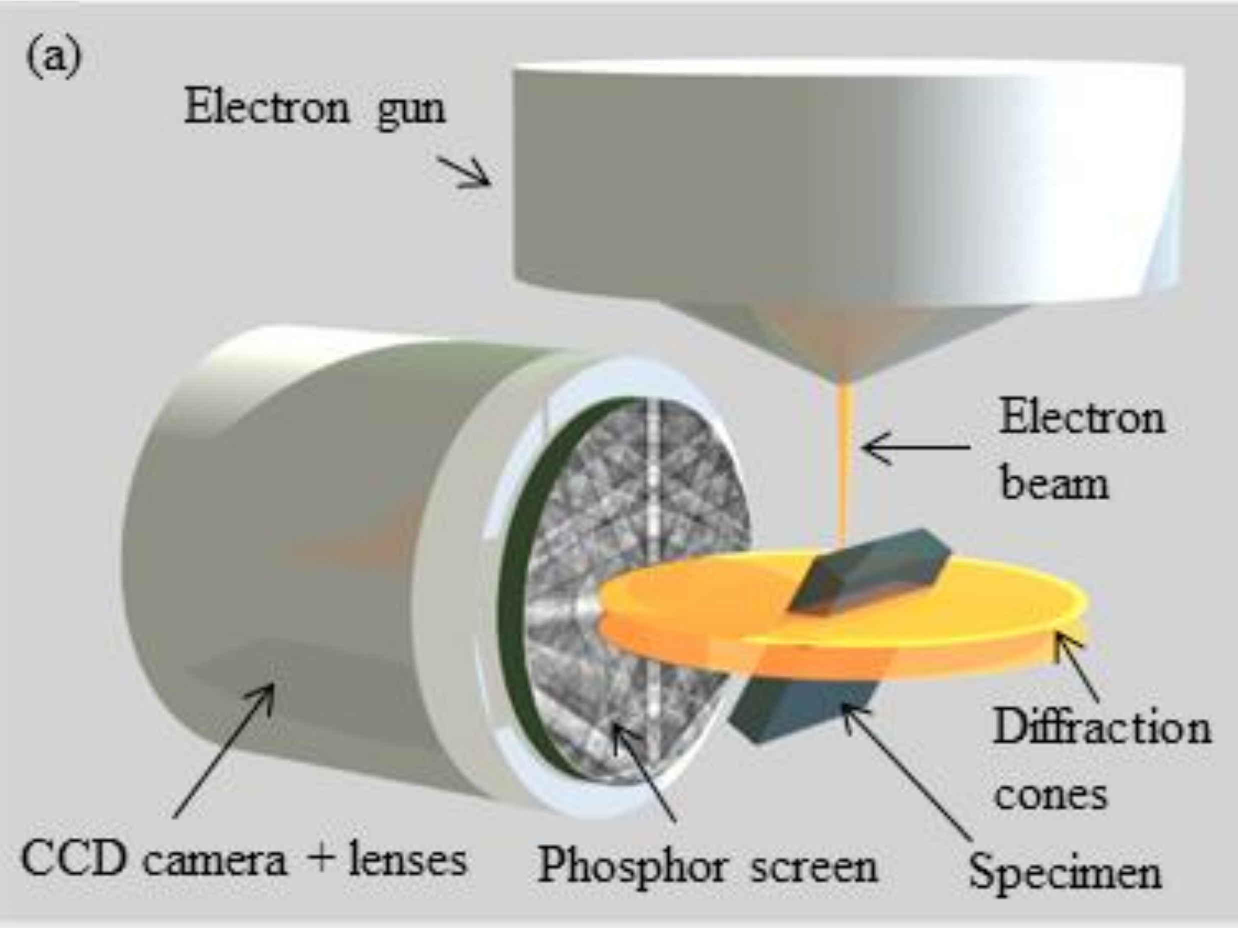

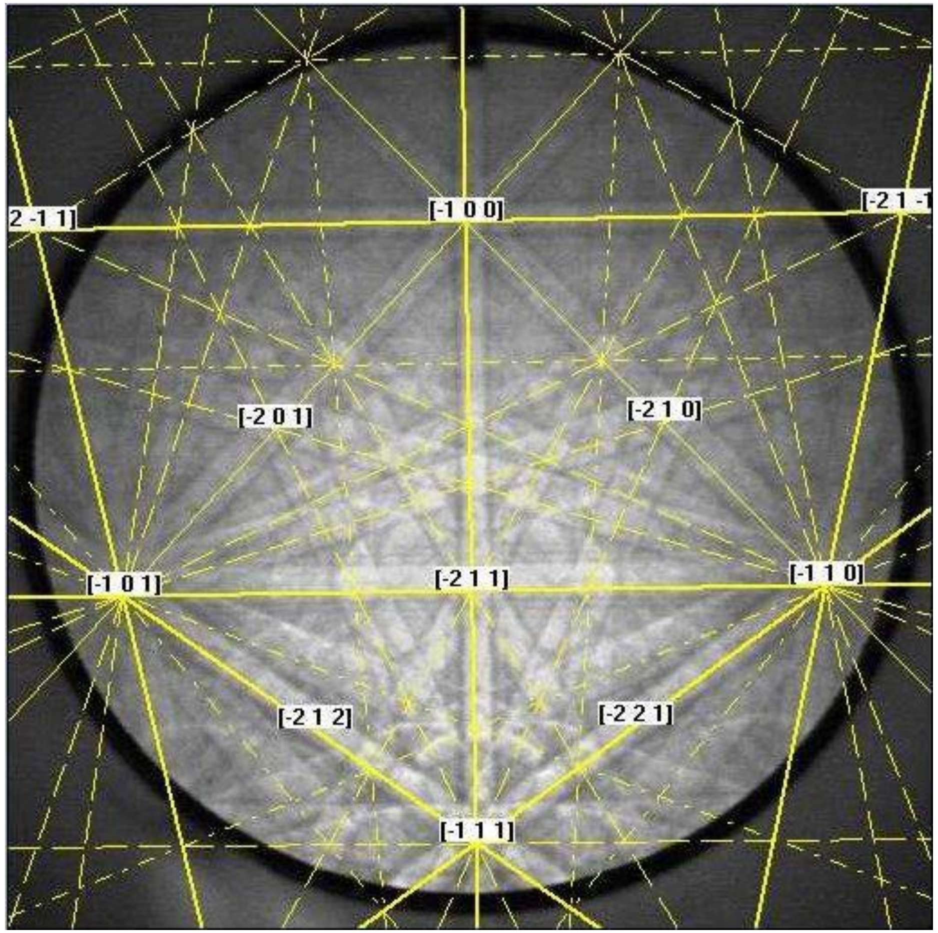

crystallographic information, crystal orientation

Examples

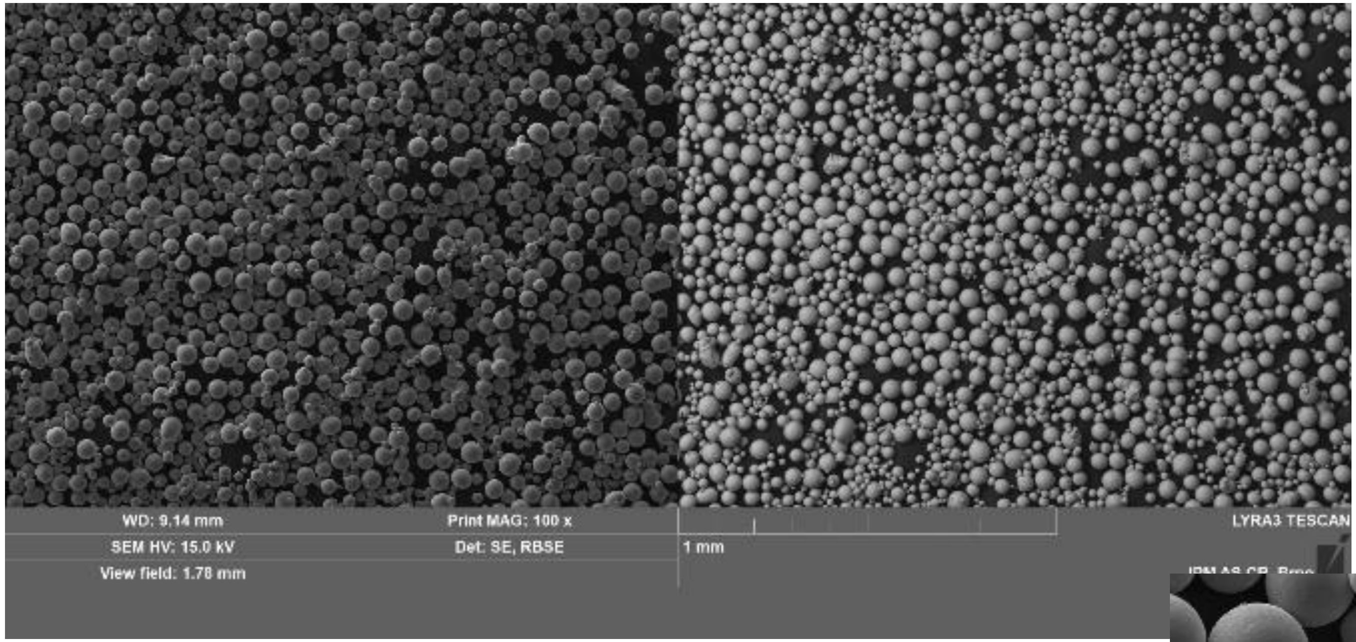

WD: 9.14 mm
Print MAG: 100 x
LYRA3 TESCAN
SEM HV: 15.0 kV
Det: SE, RBSE
1 mm
View field: 1.78 mm

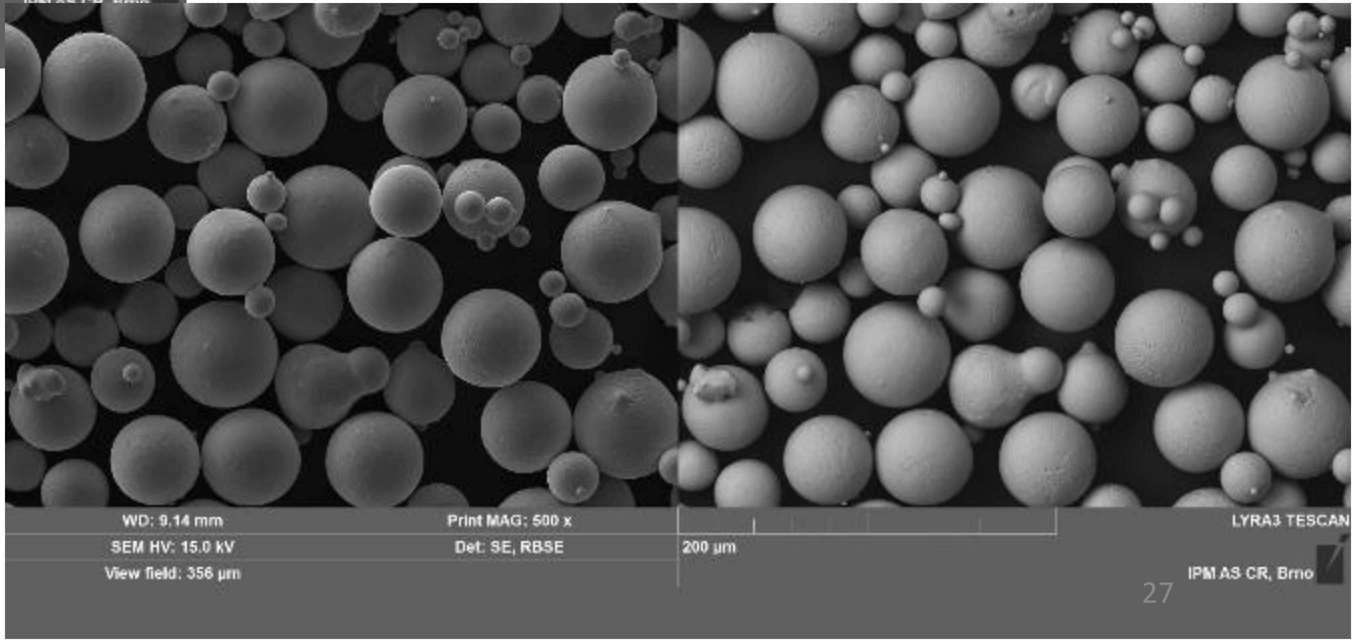

WD: 9.14 mm
Print MAG: 500 x
LYRA3 TESCAN
SEM HV: 15.0 kV
Det: SE, RBSE
200 µm
View field: 356 µm
IPM AS CR, Brno

Examples

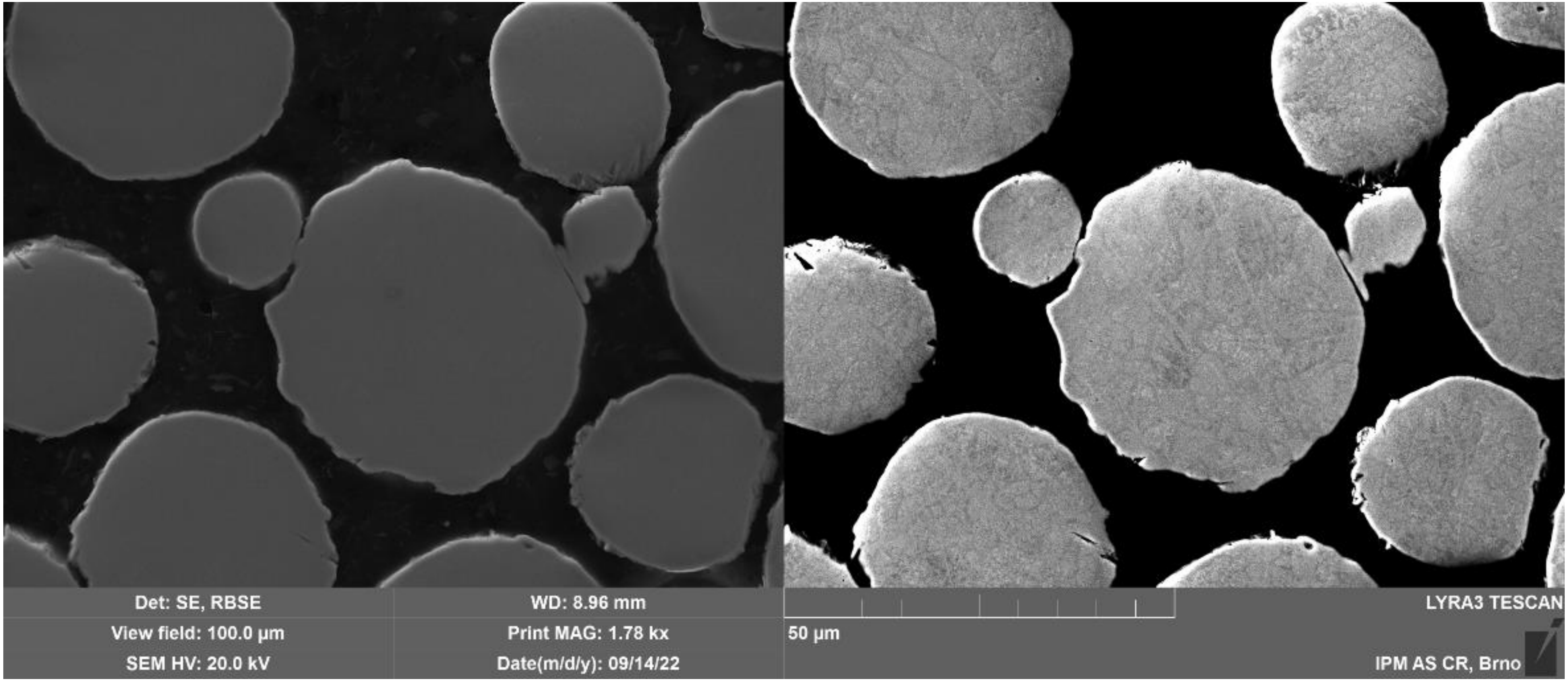
Det: SE, RBSE
View field: 100.0 µm
SEM HV: 20.0 kV
WD: 8.96 mm
Print MAG: 1.78 kx
Date(m/d/y): 09/14/22
50 µm
LYRA3 TESCAN
IPM AS CR, Brno

Examples

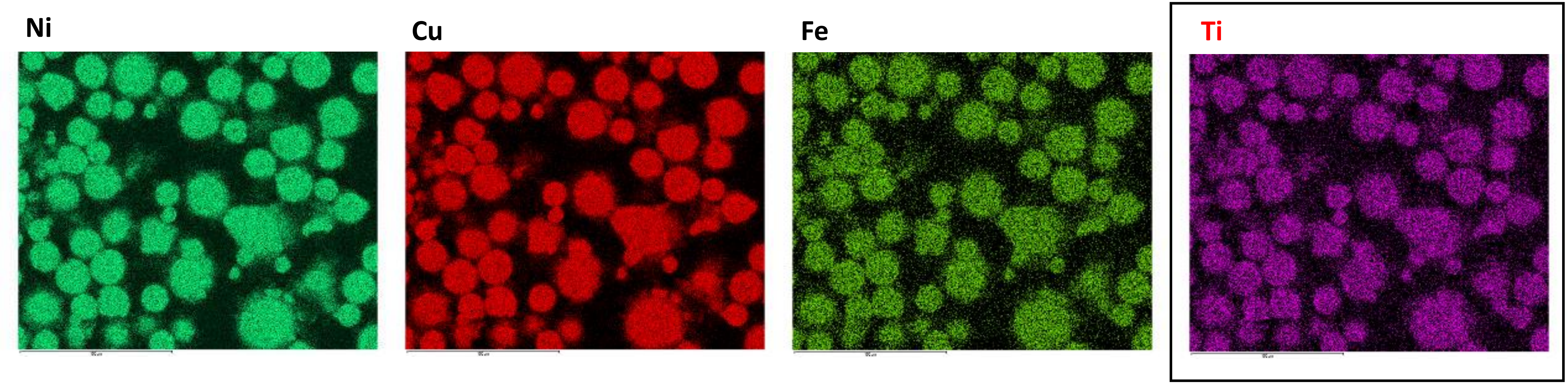
Ni
Cu
Fe
Ti

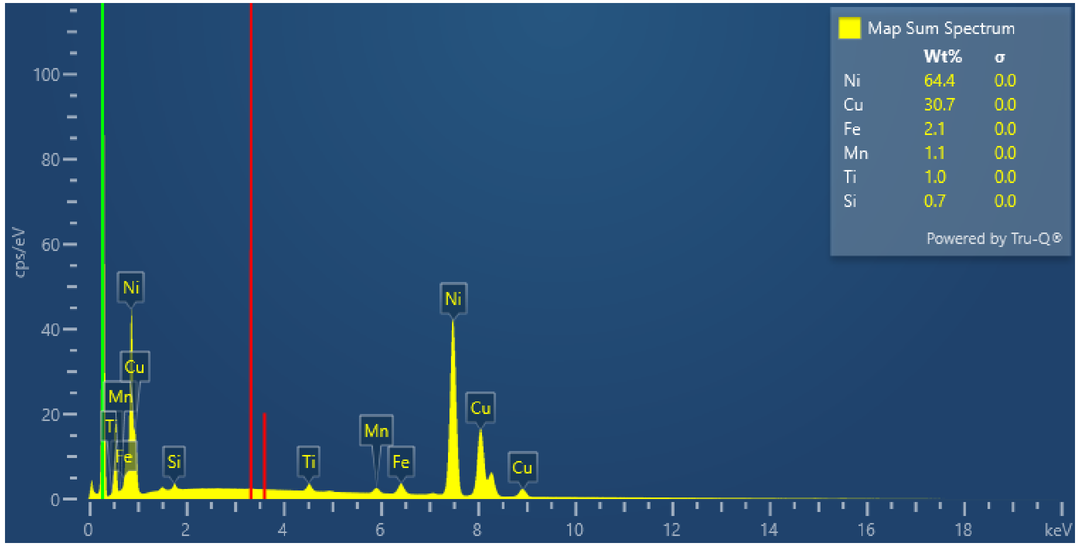
Map Sum Spectrum
Wt% σ
Ni 64.4 0.0
Cu 30.7 0.0
Fe 2.1 0.0
Mn 1.1 0.0
Ti 1.0 0.0
Si 0.7 0.0
Powered by Tru-Q®
cps/eV
keV
Ni
Cu
Mn
Ti
Fe
Si

Examples

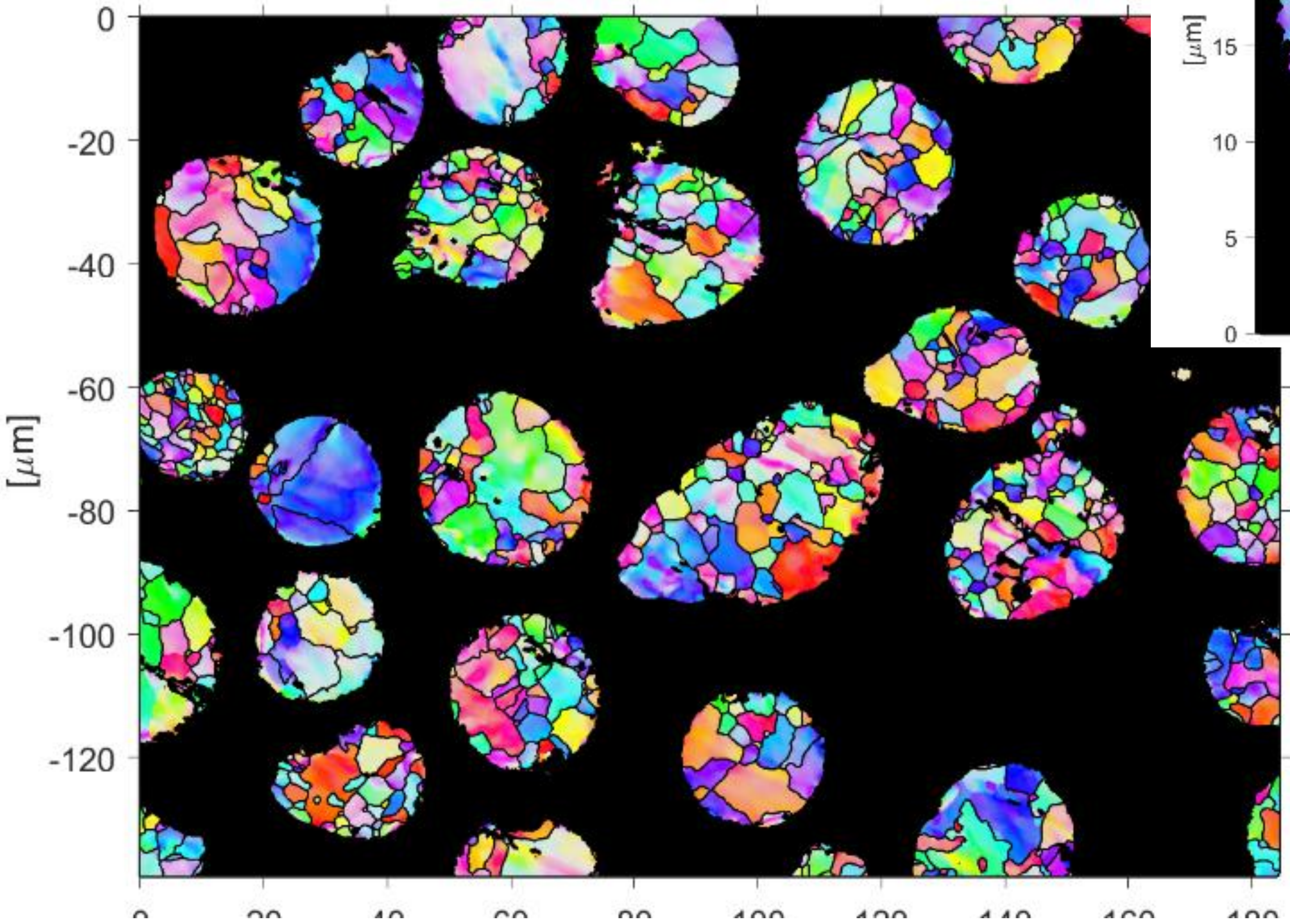

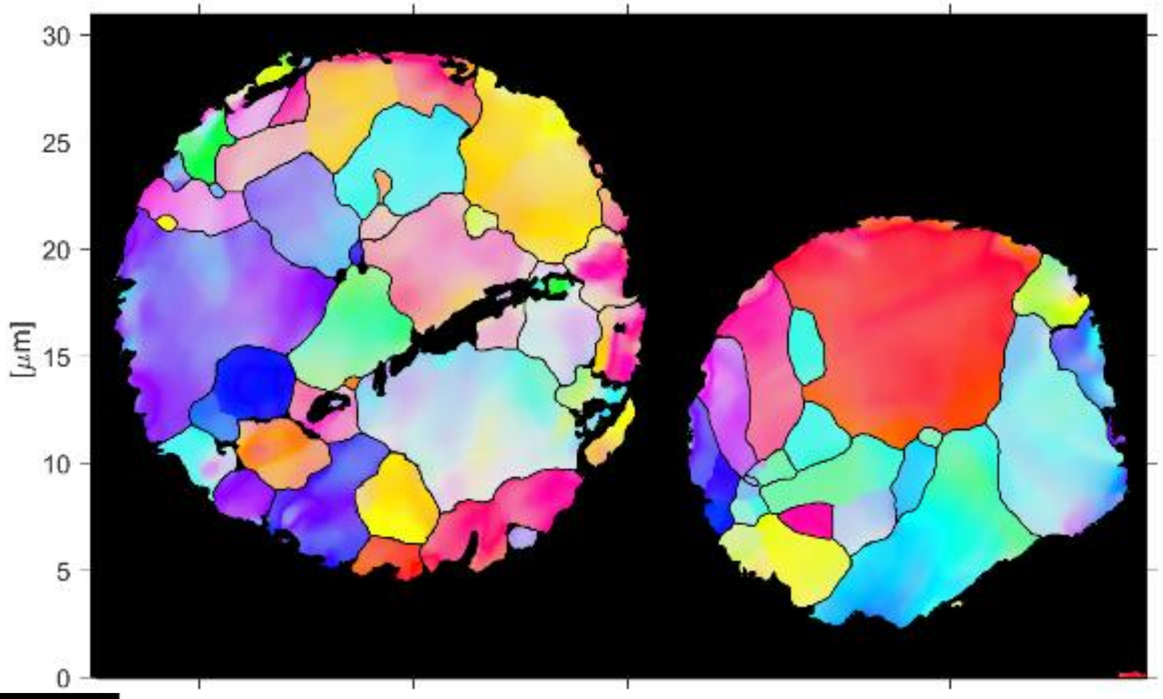

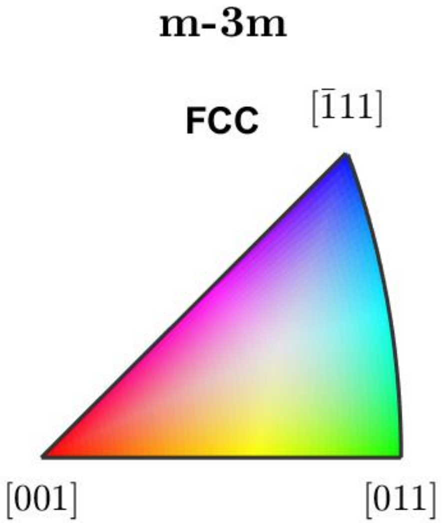

Examples

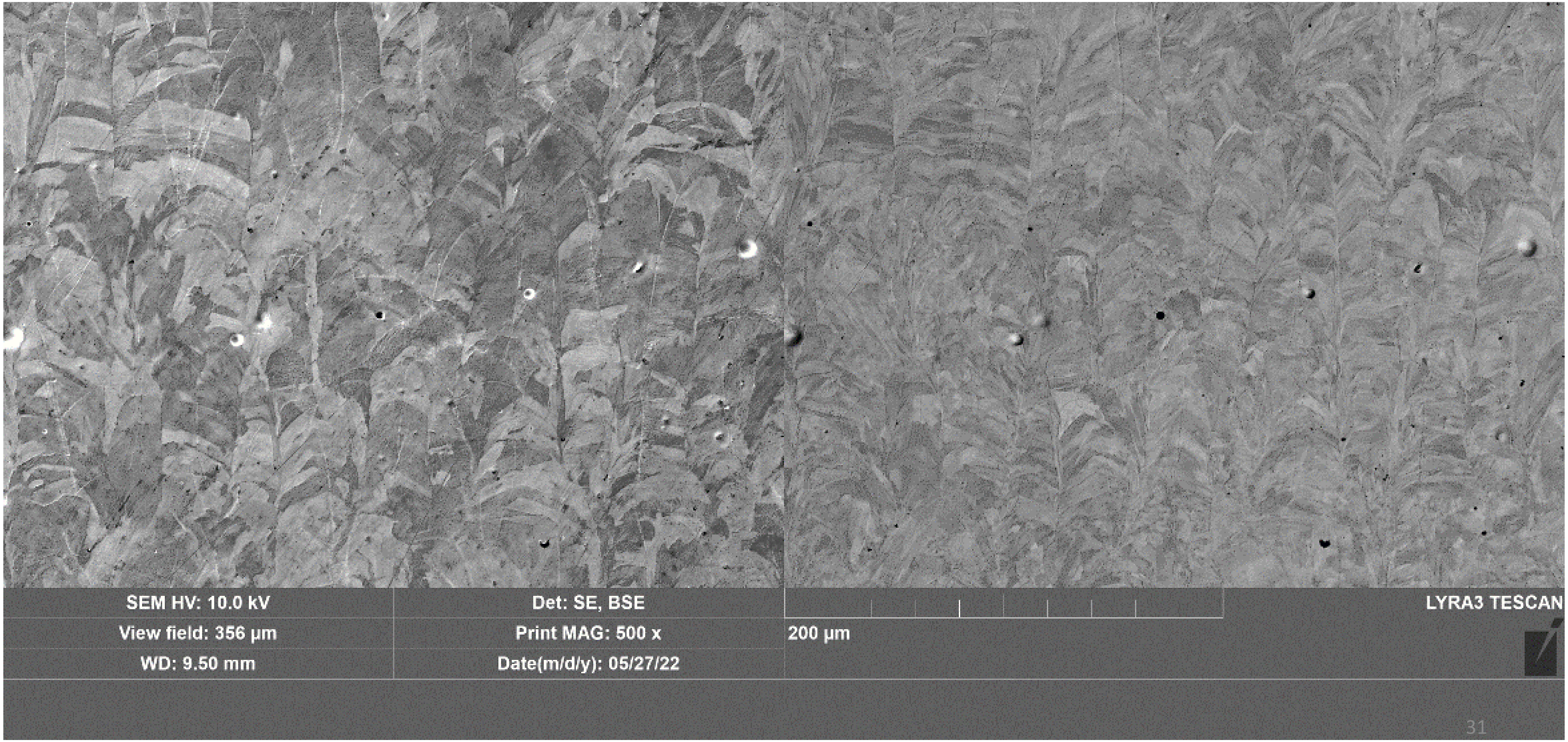
SEM HV: 10.0 kV
View field: 356 μm
WD: 9.50 mm
Det: SE, BSE
Print MAG: 500 x
Date(m/d/y): 05/27/22
200 μm
LYRA3 TESCAN

Examples

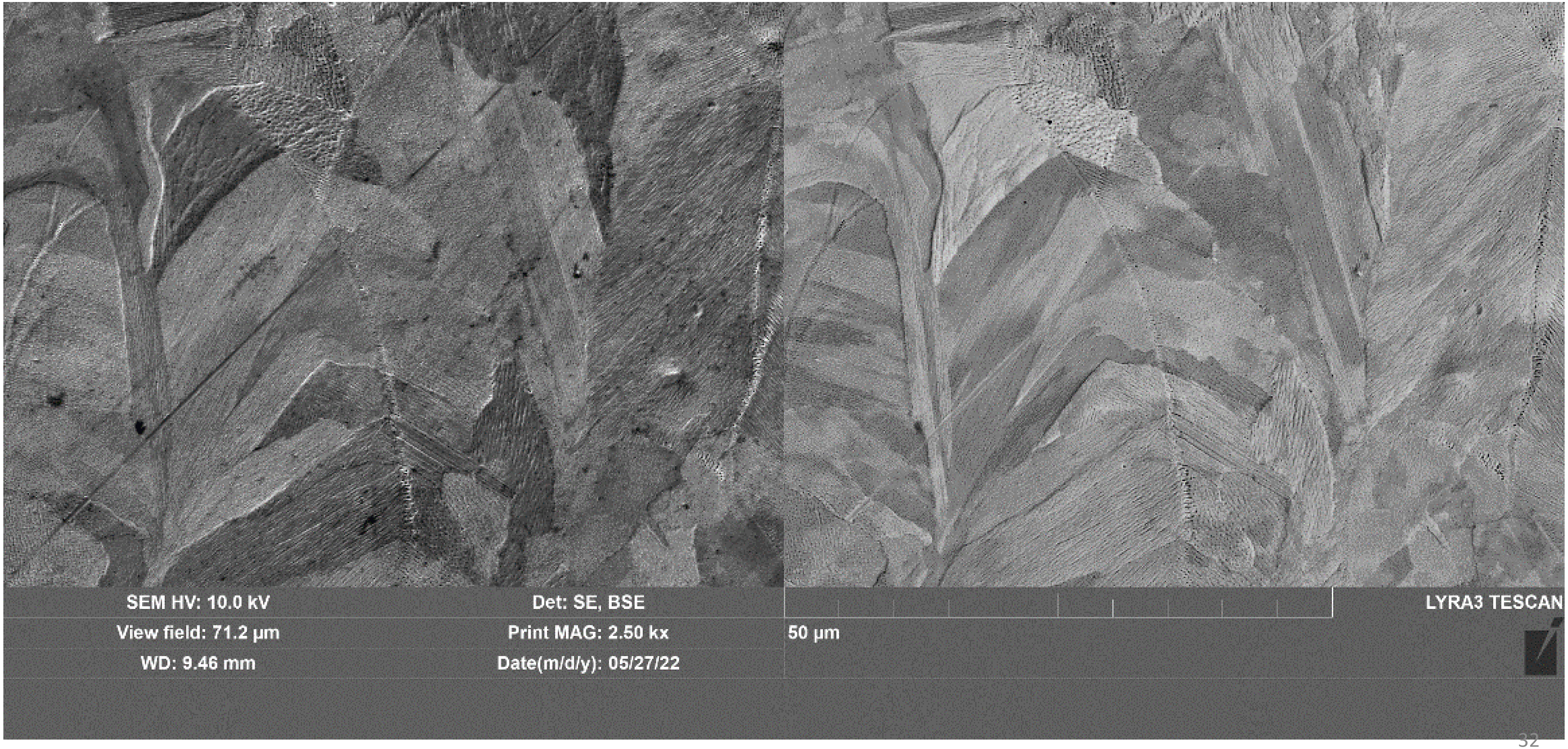
SEM HV: 10.0 kV
Det: SE, BSE
LYRA3 TESCAN
View field: 71.2 µm
Print MAG: 2.50 kx
50 µm
WD: 9.46 mm
Date(m/d/y): 05/27/22

Examples

Band contrast

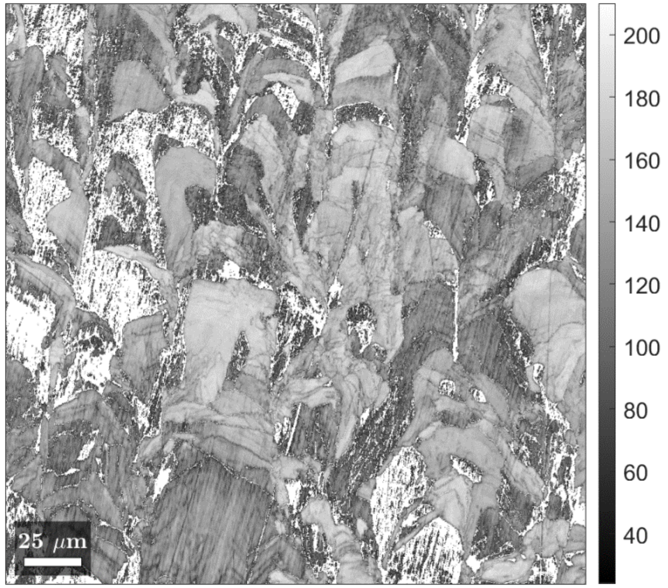

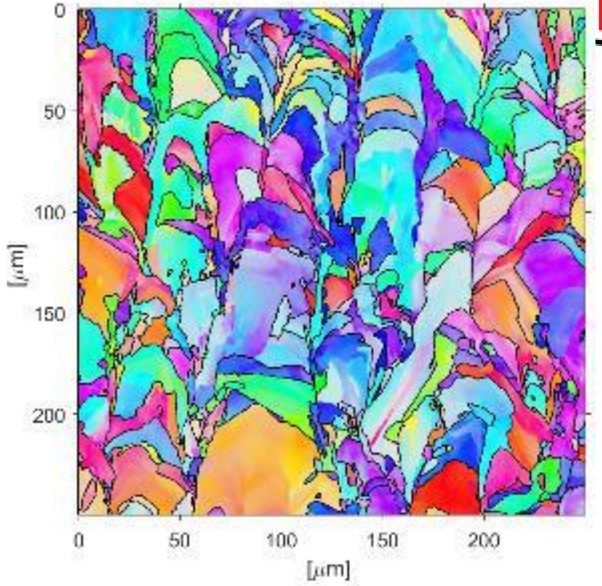

Map Z

Map Y

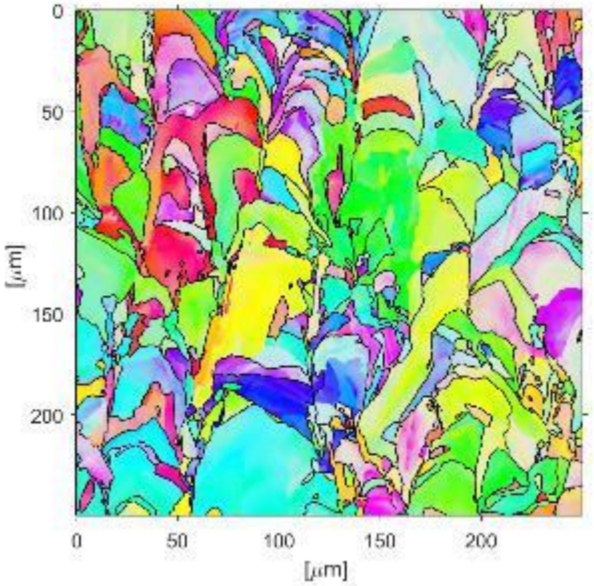

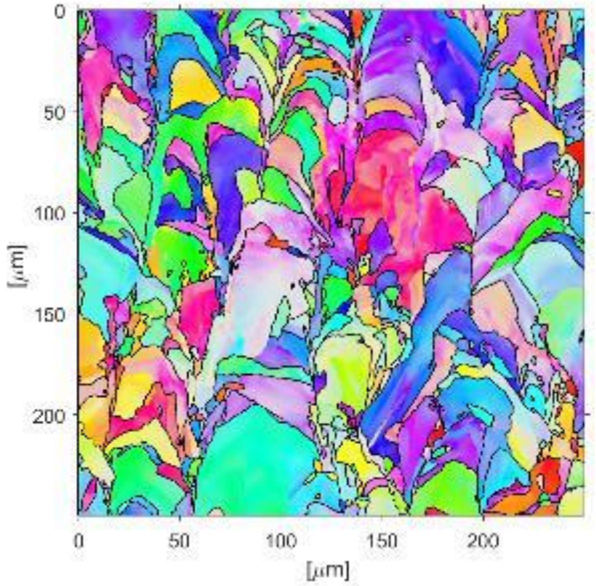

Map X

Transmission electron microscopy - diffraction

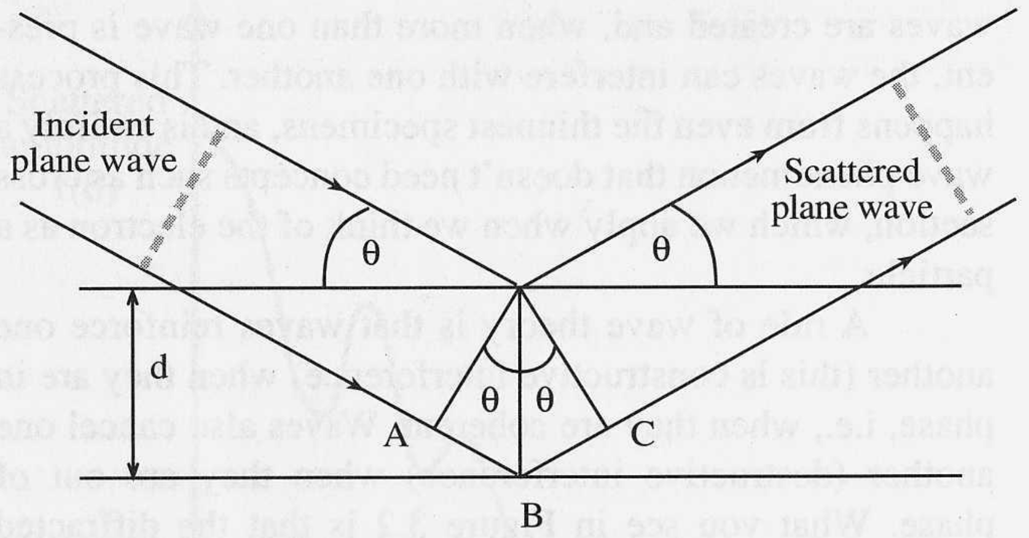

Figure 3.9. The Bragg description of diffraction in terms of the reflection of a plane wave (wavelength λ) incident at an angle θ to atomic planes of spacing *d*. The path difference between reflected waves is AB + BC.

Bragg law

$$2d_{hkl}\sin\theta = n\lambda$$

Diffraction - reciprocal space

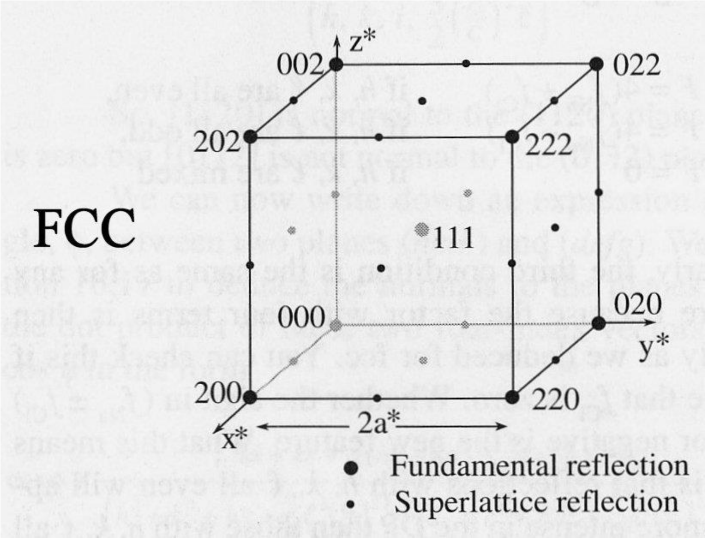

Diffraction is a 2D cut of crystal in reciprocal space

Cubic, tetragonal and orthorhombic lattice

$\boldsymbol{a}^* \parallel \boldsymbol{a} \qquad \boldsymbol{b}^* \parallel \boldsymbol{b} \qquad \boldsymbol{c}^* \parallel \boldsymbol{c}$

$a^* = 1/a \qquad b^* = 1/b \qquad c^* = 1/c$

$\alpha^* = \beta^* = \gamma^* = \pi/2$

Hexagonal and trigonal lattice

$\boldsymbol{c}^* \parallel \boldsymbol{c} \qquad \boldsymbol{a}^* \text{ and } \boldsymbol{b}^* \in (\boldsymbol{a}, \boldsymbol{b})$

$a^* = b^* = 2/(a\sqrt{3}) \qquad c^* = 1/c$

$\alpha^* = \beta^* = \pi/2 \qquad \gamma^* = \pi/3$

Diffraction patterns – single crystal / one grain

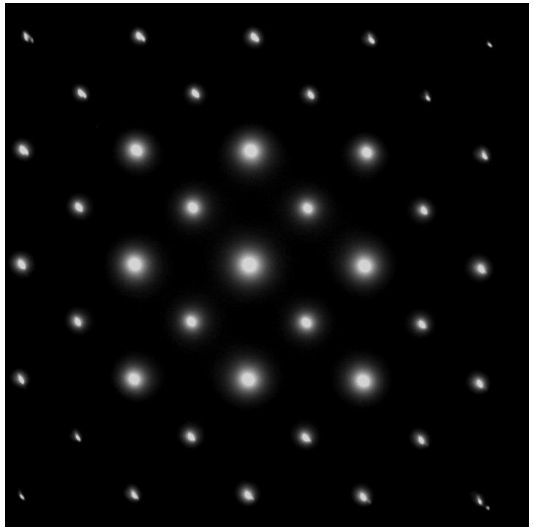
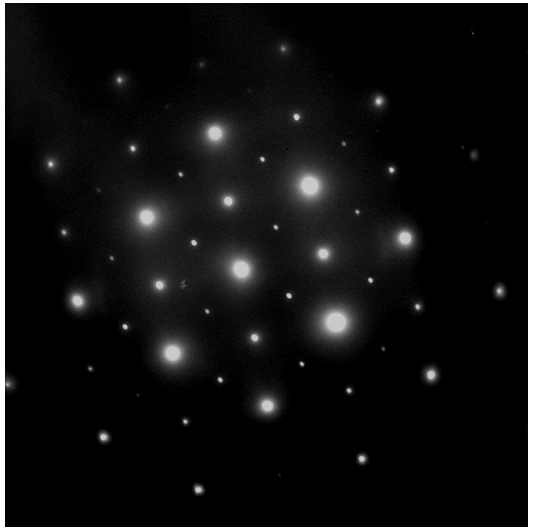
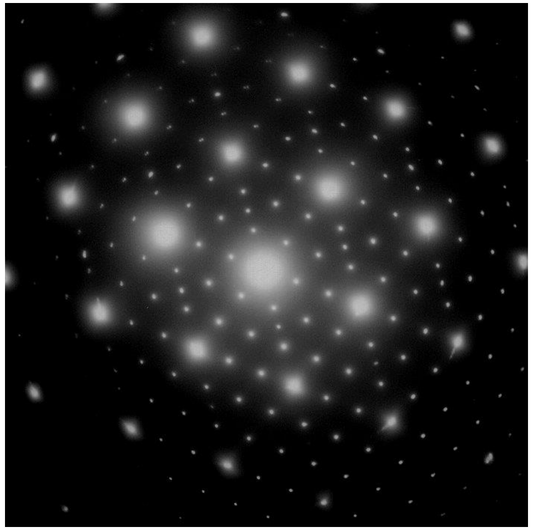
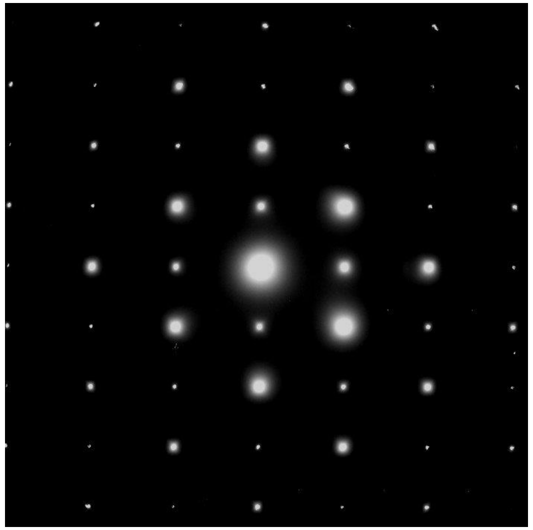
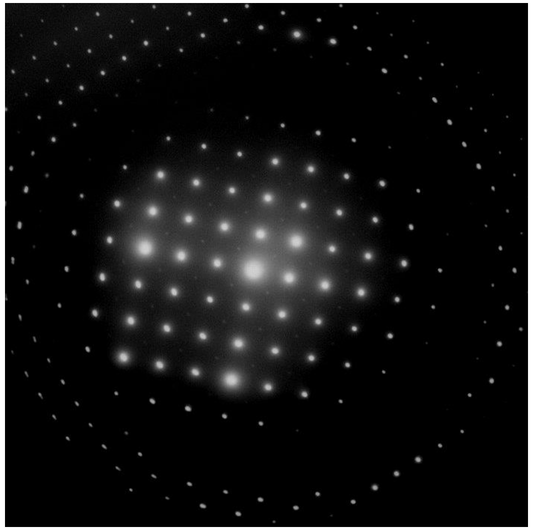
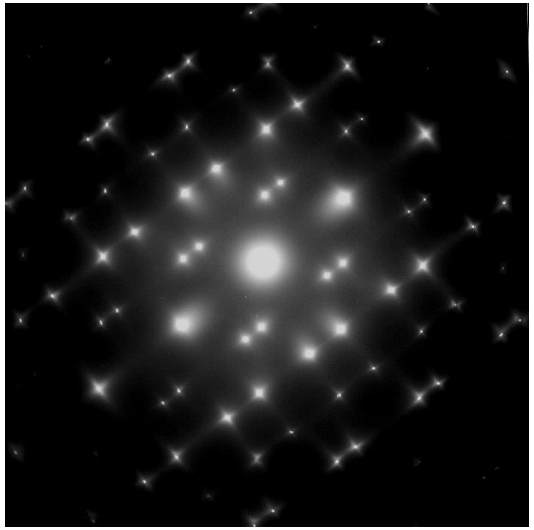

Diffraction patterns

Nanocrystals

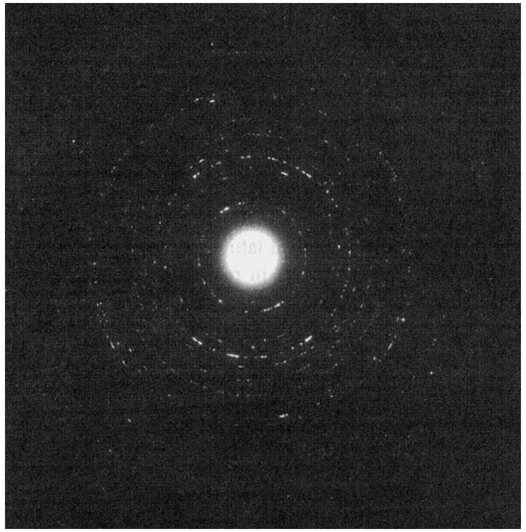

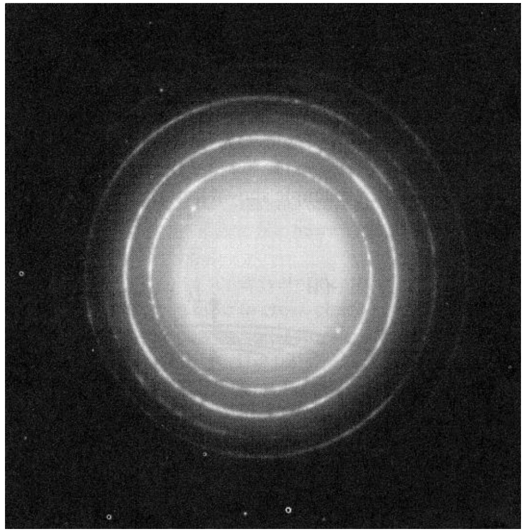

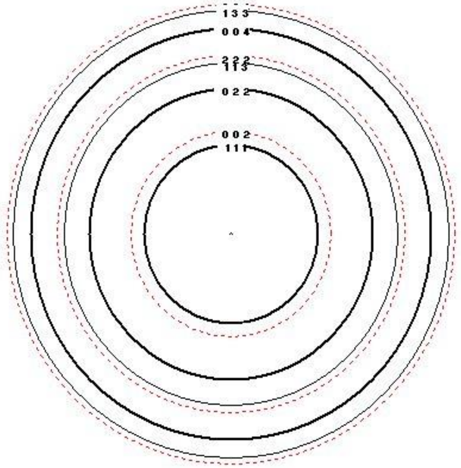

Amorphous

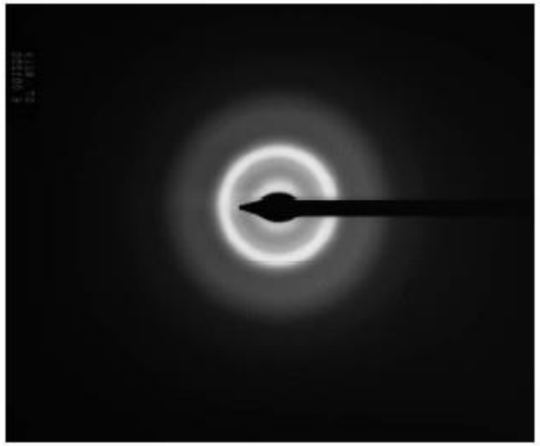

Fig. 3. Electron diffraction pattern taken from the cross section of the 2 mm thick $Cu_{64}Zr_{36}$ cast strip. Same result across the whole specimen.

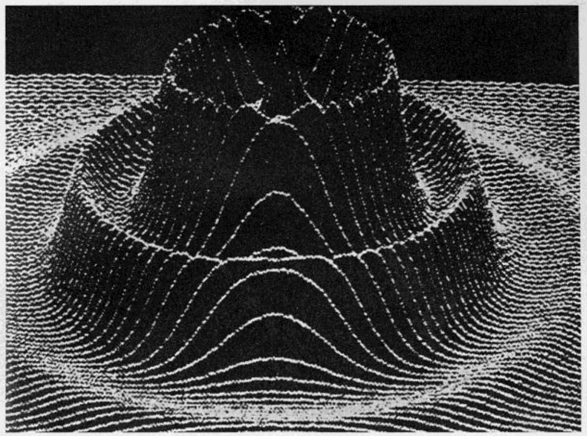

Figure 18.13. A computer plot of the diffracted-intensity distribution from an amorphous structure, showing diffuse rings of intensity. The direct-beam intensity is off scale.

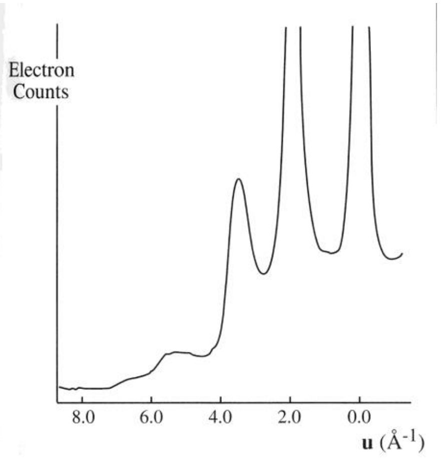

Figure 18.12. An intensity profile across an energy-filtered diffraction pattern from amorphous Si obtained by scanning the pattern across the entrance slit to a serial EELS spectrometer and recording only the elastic (on-axis) electrons.

Transmission electron microscopy – Imagining

$$d\psi_g = i\lambda \frac{F_g n}{\cos\theta} e^{2\pi i \vec{k}\cdot\vec{r}} \equiv q$$

Kinematic approximation

$$\Phi_g = \int_0^t d\Phi_g = \frac{i\pi}{\xi_g}\frac{\sin(\pi t s_g)}{\pi s_g}\exp(-\pi i s_g t), \longrightarrow \mathrm{I_g} \propto \frac{\sin^2(\pi t s_g)}{(s_g \xi_g)^2}$$

Dynamic theory

$$\frac{d\Phi_g(z)}{dz} = \frac{\pi i}{\xi_0}\Phi_g(z) + \frac{\pi i}{\xi_g}\Phi_0(z)\exp(2\pi i(\vec{\chi} - \vec{\chi}')\cdot\vec{r})$$

$$\frac{d\Phi_0(z)}{dz} = \frac{\pi i}{\xi_0}\Phi_0(z) + \frac{\pi i}{\xi_g}\Phi_g(z)\exp(2\pi i(\vec{\chi}' - \vec{\chi})\cdot\vec{r})$$

quite complicated….

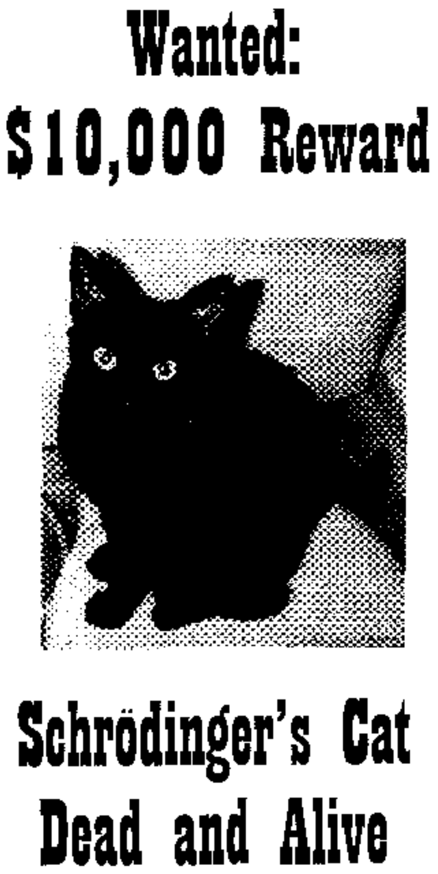

Transmission electron microscopy – Imagining

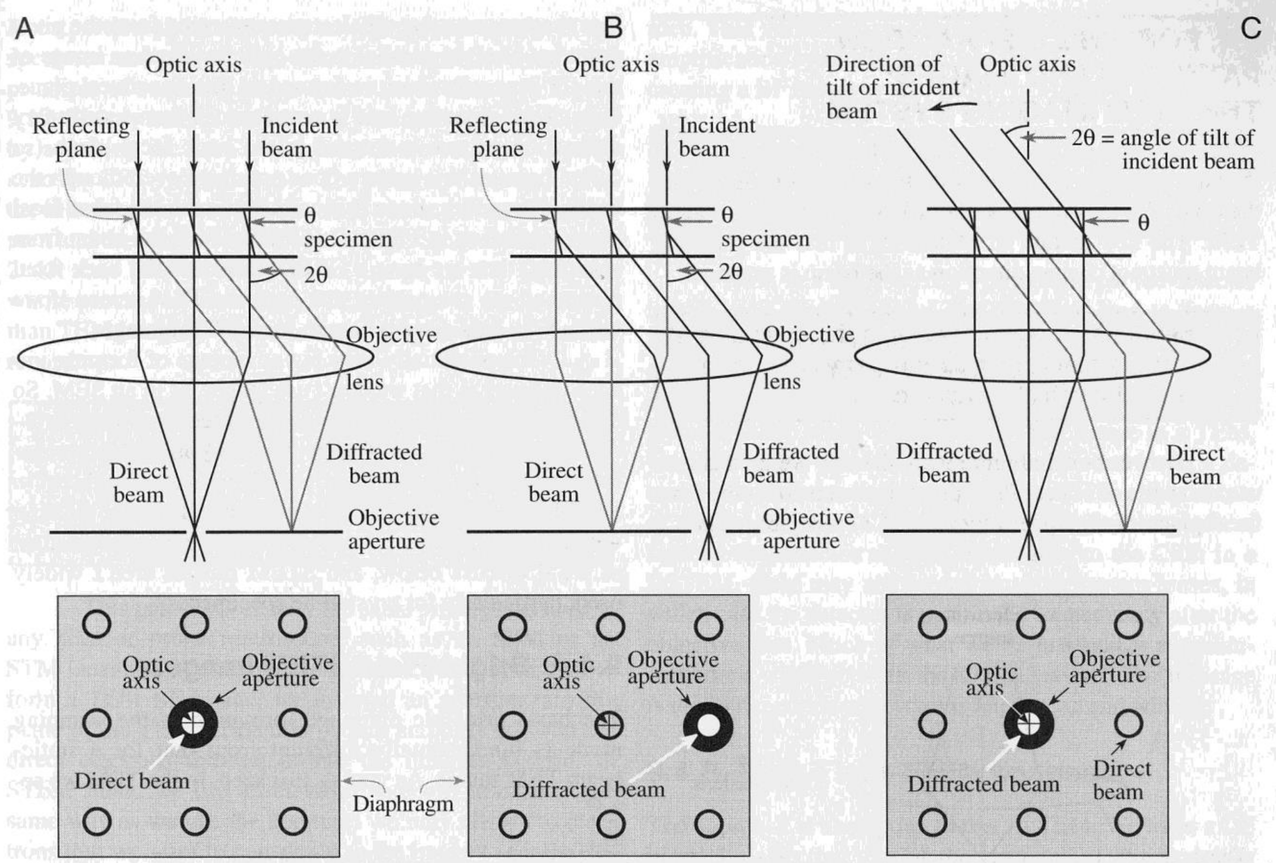

Figure 9.14. Ray diagrams showing how the objective lens/aperture are used in combination to produce (A) a BF image formed from the direct beam, (B) a displaced-aperture DF image formed with a specific off-axis scattered beam, and (C) a CDF image where the incident beam is tilted so that the scattered beam remains on axis. The area selected by the objective aperture, as seen on the viewing screen, is shown below each ray diagram.

TEM – Monel – FIB lamella

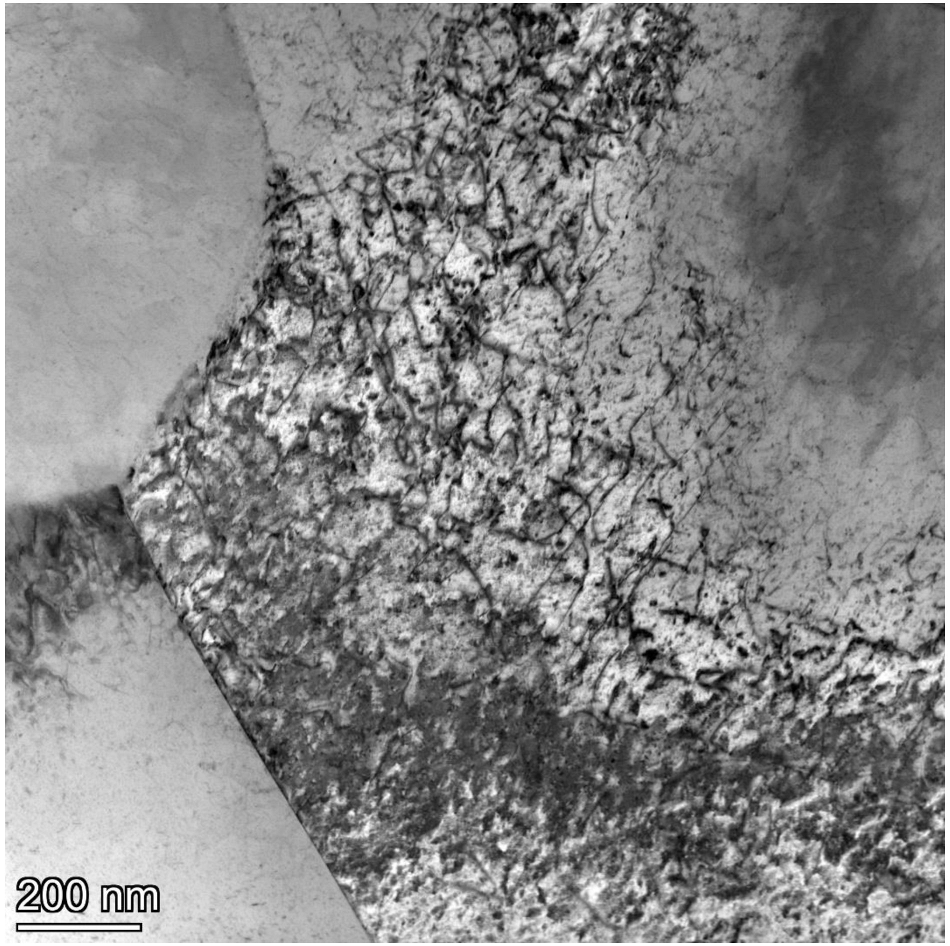

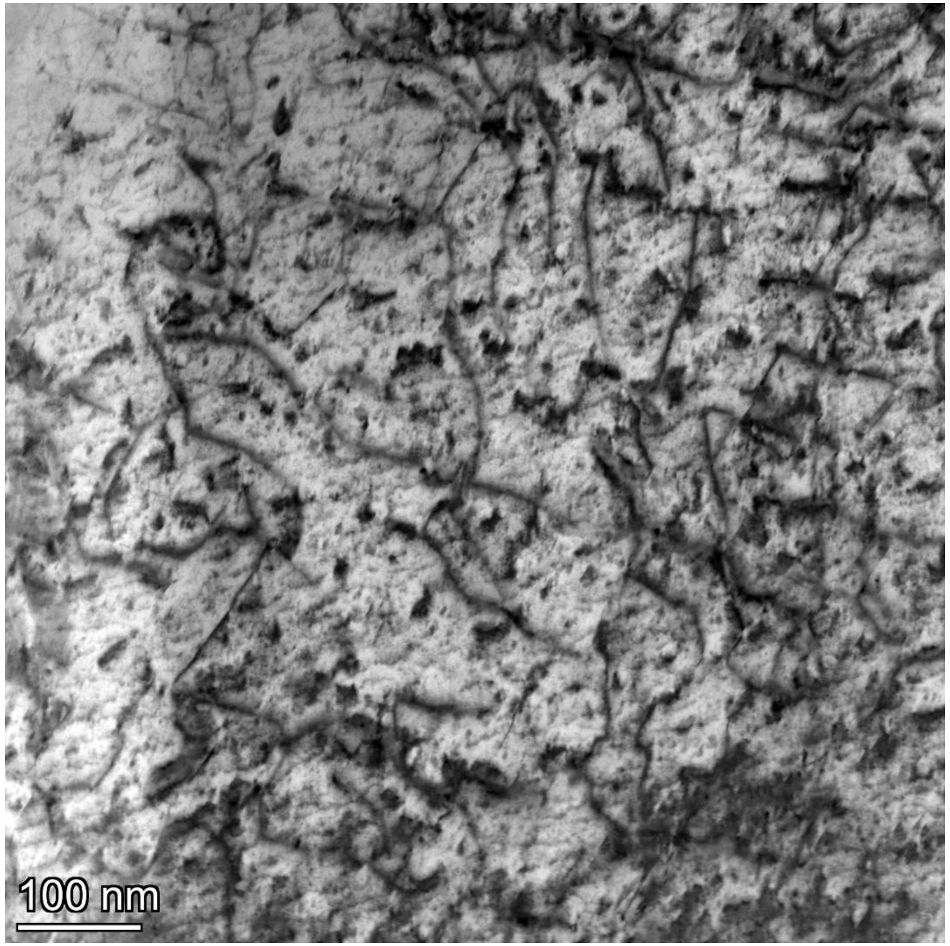

Very high dislocation density. Black dots are probably prizmatic dislocation loops

TEM – Kanthal powder

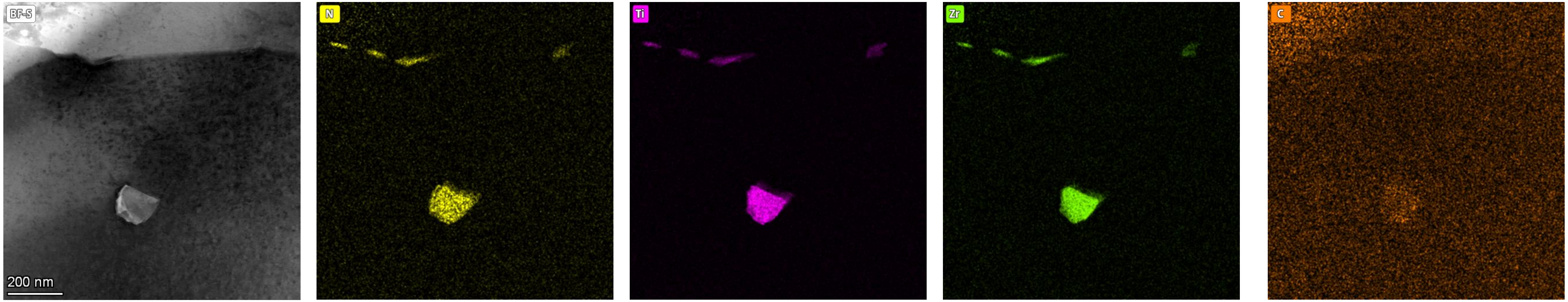

TEM – Monel - bulk

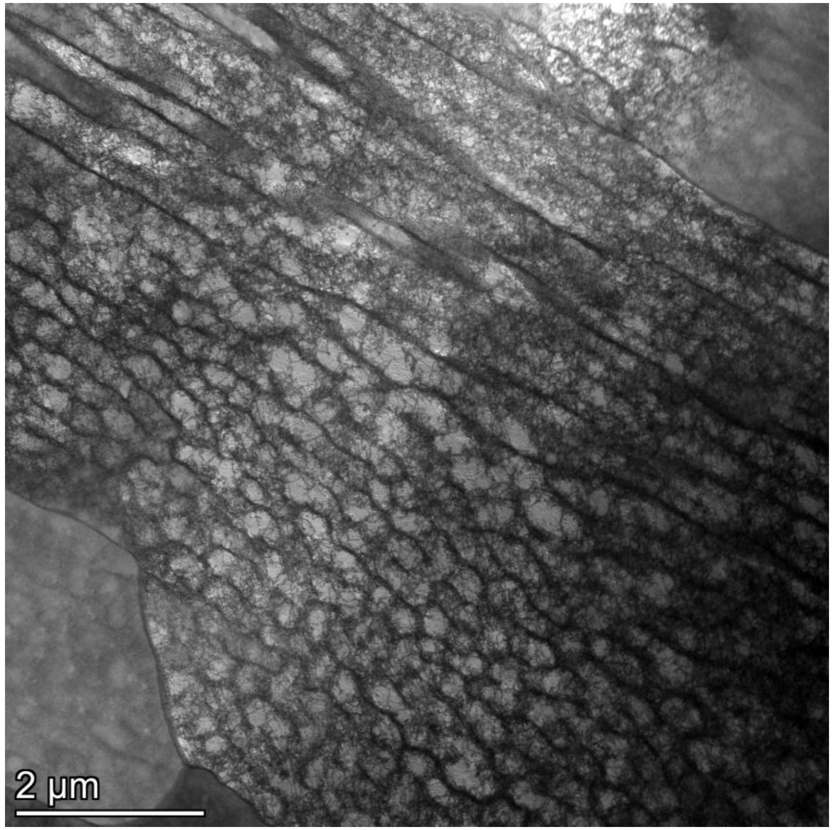

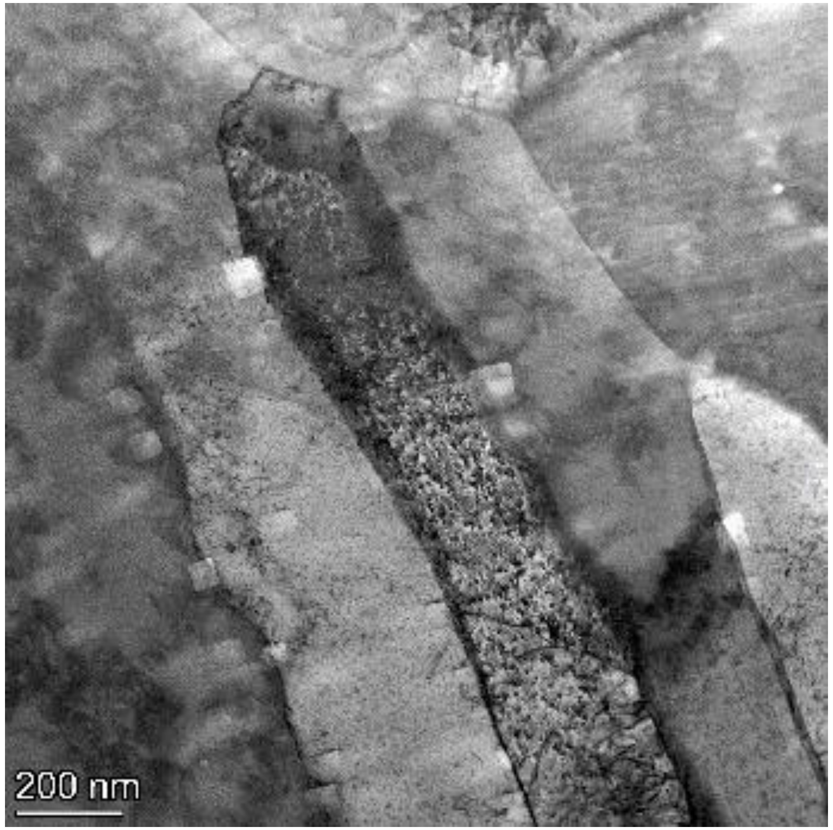

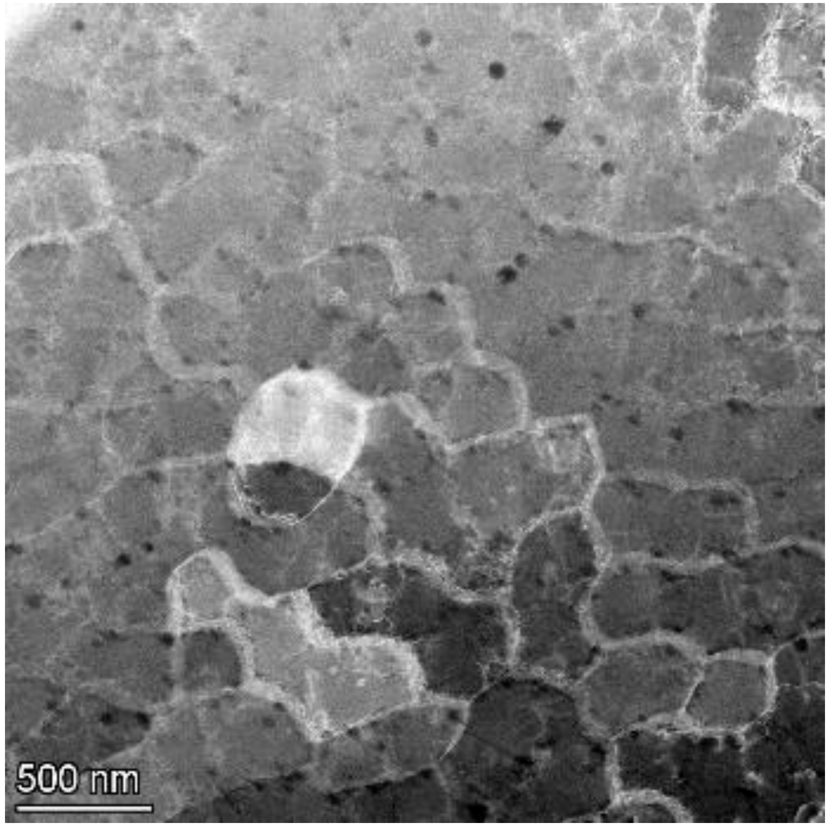

Cold spray - austenitic steel

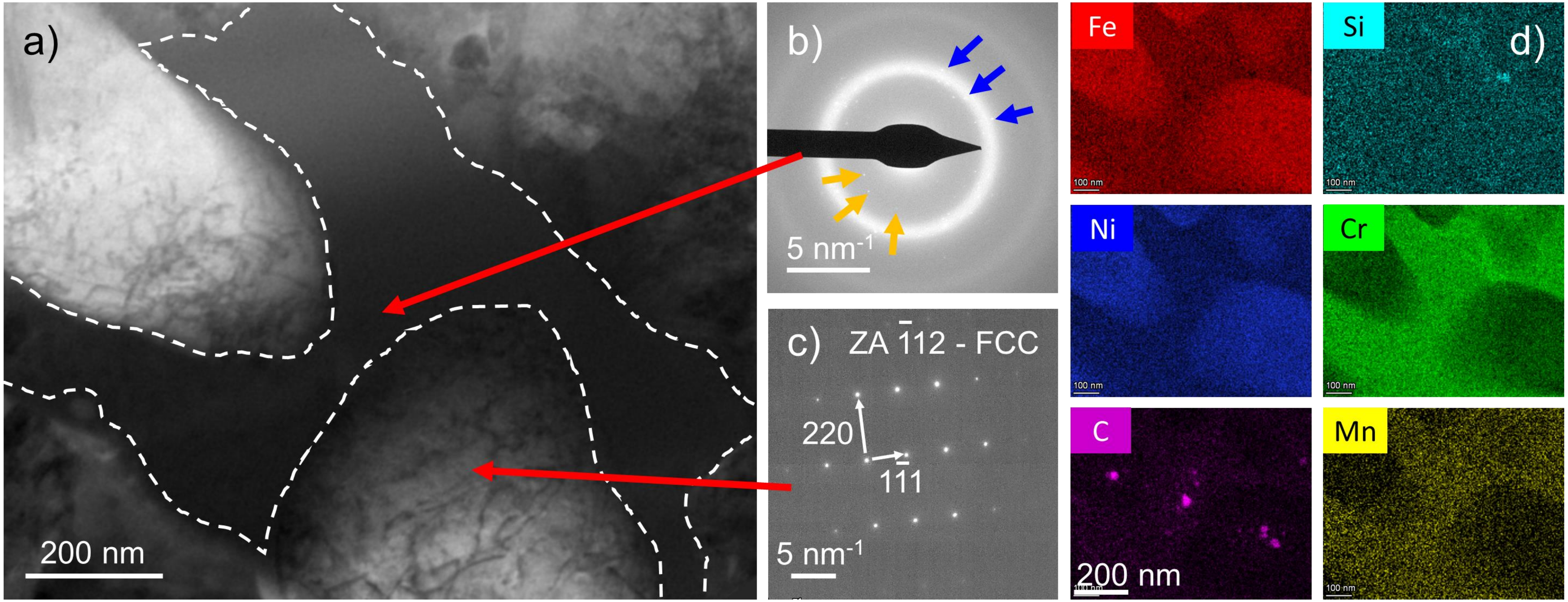

Cold spray - austenitic steel